ADDIS ABABA UNIVERSITY

SCHOOL OF GRADUATE STUDIES

ADDIS ABABA INSTITUTE OF TECHNOLOGY

SCHOOL OF ELECTRICAL AND COMPUTER ENGINEERING

Comparative Analysis of Non-Blind Algorithms on the basis of Sidelobe Level for Smart Antenna System

By

Seid Ahmed

Advisor

Dr. Murad Ridwan

A Thesis Submitted to the School of Graduate Studies of Addis Ababa University in Partial Fulfillment of the Requirements for the Degree of Masters of Science in Electrical Engineering

July, 2018

Addis Ababa, Ethiopia

ADDIS ABABA UNIVERSITY

SCHOOL OF GRADUATE STUDIES

ADDIS ABABA INSTITUTE OF TECHNOLOGY

SCHOOL OF ELECTRICAL AND COMPUTER ENGINEERING

Comparative Analysis of Non-Blind Algorithms on the basis of Sidelobe Level for Smart Antenna System

By

Seid Ahmed

Approved by board of examiners

_____	_____	_____
Chairman, Dept. Graduate Committee	Signature	date
_____	_____	_____
Advisor	Signature	date
_____	_____	_____
Internal Examiner	Signature	date
_____	_____	_____
External Examiner	Signature	date

Abstract

From time to time the need for good quality communication is required in different aspects of life. Many challenges can face service providers for implementing different communication facilities. One of these great challenges is the limitation of available radio frequency. So it is mandatory to use the scarce resource most efficiently in parallel with providing good quality of service for the customers. One of the way, for efficient utilization of limited radio frequency (RF) spectrum is to use smart antenna system. Smart antenna radiates not only narrow beam towards desired users exploiting signal processing capability but also places null towards interferers, thus optimizing the signal quality and enhancing capacity.

The efficiency of the smart antenna can depend on different parameters like angle of separation between the desired and the interferer signal, the number of elements of the array and the spacing between the array elements. Different researches showed that the performance of smart antenna can be improved by using an array with a relatively large number of elements having an optimum spacing between them with a relatively large angle of separation between the desired and the interferer signal.

The central aim of this thesis work is comparing the performance of smart antenna in terms of reducing radiation in unintended direction. This is achieved by using an algorithm that produces lower sidelobe level in the radiation pattern of the antenna. Comparative analysis of three non-blind algorithms, Least Mean Square (LMS), Sample Matrix Inversion (SMI) and Recursive Least Square (RLS), on the basis of Sidelobe Level (SLL) is studied in this thesis work. Smart antenna incorporates these algorithms to calculate complex weights according to the signal environment. Simulation results reveal that all the three algorithms have their own beamforming characteristics. But the LMS produces lower sidelobe level as compared to the other two algorithms. Therefore, the LMS algorithm is found the most efficient because of its simplicity, lower complexity and sidelobe level for communication through a flat fading channel. In addition, as the number of elements increases, the sidelobe level of array factor pattern decreases for the case of LMS algorithm.

Keywords: Beamforming, LMS, RLS, SMI, Sidelobe Level, smart antenna

Declaration

I, the undersigned, declare that this thesis is my original work, has not been presented for a degree in this or any other university, and all sources of materials used for the thesis have been fully acknowledged.

Seid Ahmed _____

Name Signature

Place: Addis Ababa

Date of Submission: _____

Dr. Murad Ridwan _____

Advisor's Name Signature

ACKNOWLEDGEMENT

I wish to thank Almighty Allah who gave me the strength and determination to complete this thesis. I gratefully acknowledge the continuous guidance and motivation provided to me by my advisor Dr. Murad Ridwan. Without his personal supervision, advice and help, timely completion of this thesis work would have been impossible.

My special thanks are extended to my beloved wife Kubra Siraj and to my family for their never ending patience and support for my mental peace and to my parents for the strength that they gave me through their prayers.

Finally, I wish to heartily thank staffs of the School of Electrical and Computer Engineering, AAU, all my classmates for their heartfelt cooperation and idea sharing throughout my thesis work.

Table of Contents

LIST OF FIGURES

LIST OF TABLES

LIST OF ACRONYMS

AF	Array Factor
AWGN	Additive White Gaussian Noise
CDMA	Code Division Multiple Access
CM	Constant Modulus
DBF	Digital Beam Former
DD	Decision Directed
DOA	Direction of Arrival
ESPRIT	Estimation of signal parameters via rotational invariance techniques
FDMA	Frequency Division Multiple Access
LMS	Least Mean Square
MLM	Maximum Likelihood Method
MMSE	Minimum Mean Square Error
MSE	Mean Square Error
MSINR	Maximum Signal-to-Interference plus Noise Ratio
MUSIC	Multiple Signal Classification
MVDRE	Minimum Variance Distortionless Response Estimator
QoS	Quality of Service
RF	Radio Frequency
RLS	Recursive Least Squares
SCORE	Spectral self-Coherence Restoral
SDMA	Space Division Multiple Access
SINR	Signal-to- Interference plus Noise Ratio
SIR	Signal to Interference Ratio
SLL	Side Lobe Level
SMI	Sample Matrix Inversion
SNR	Signal to Noise Ratio
TDMA	Time Division Multiple Access
ULA	Uniform Linear Array

Chapter 1: Introduction

1.1 Background

Global demand for voice, data and video related services continues to grow faster than the required infrastructure can be deployed. Despite huge amount of money that has been spent in attempts to meet the need of the world market, the vast majority of people on Earth still do not have access to quality communication facilities. The greatest challenge faced by governments and service providers is the "last-mile" connection, which is the final link between the individual home or business users and worldwide network. Copper wires, traditional means of providing this "last-mile" connection is both costly and inadequate to meet the needs of the bandwidth intensive applications. Coaxial cable and power line communications all have technical limitations. And fiber optics, while technically superior and widely used in backbone applications, is extremely expensive to install to every home or business user. This is why more and more the wireless connection is being seen as an alternative to quickly and cost effectively meeting the need for flexible broadband links [1].

In most wireless communications systems, there are two major components - base stations and the mobiles. The base station is located at the center of a coverage area called a 'cell' and the mobiles can be anywhere within the cell. Communication then takes place between the base station and the mobile through the wireless channel. A certain amount of spectrum is assigned to a cell for signal transfer. Since the available spectrum for any service provided by operator is limited, different mechanisms of spectrum multiple access techniques has been evolved for increasing capacity of mobile communication system with the available bandwidth.

It is always a challenge to provide higher system capacity in the network to fulfill the growing demand. One recent development in this area is a use of smart antenna with MA also known as Space Division Multiple Access (SDMA) technology [2].

Space Division Multiple Access: - In this type of multiple access technique, users are separated by their spatial locations. In a regular base station, the antenna is either Omni-directional or sectorized in which the radiation pattern is fixed in either all direction or in a sector portion of the cell which wastes a lot of energy due to the fact that the mobile being addressed can only occupy

one spot at a time. It also creates undesired interference to other users located with the cell. But the smart antenna radiation pattern directs the beam towards the users of interest only & nulls toward interference to improve the capacity of cellular system.

There are two basic types of smart antenna systems.

1) Switched beam antenna system: -form multiple fixed beams with heightened sensitivity in particular directions. These antenna systems detect signal strength, choose from one of several predetermined, fixed beams, and switch from one beam to another as demand changes throughout the sector.

2) Adaptive antenna array system: - represent the most advanced smart antenna approach to date. Using a variety of new signal-processing algorithms, the adaptive system takes advantage of its ability to effectively locate and track various types of signals to dynamically minimize interference and maximize intended signal reception [3]. In doing so the Signal-to-Noise Ratio will be maximized and the capacity of the system for the desired user can be improved.

1.2 Review of related works

Researches were done on the use of smart antenna based on different perspective for increasing capacity and reducing interference level of the antenna in mobile communication system.
Among these include:

G. V. Tsoulos, M. A. Beach, and S. C. Swales, on the title “Application of Adaptive Antenna Technology to Third Generation Mixed Cell Radio Architectures," shows that adaptive antennas could improve spectral efficiency by up to 15% in a CDMA system with overlaid macro, micro, and pico cells [4].

U. Forsse'n, J. Karlsson, B. Johannisson, M. Almgren, F. Lotse, and F. Kronestedt on the title "Adaptive Antenna Arrays for GSM900” A 10 element scanned beam array is compared with a 120-degree sector antenna. The channel model includes Rayleigh fading, log-normal shadowing with $\sigma = 6$ dB, a Doppler shift of 2.5 Hz, and path loss exponent $\gamma = 35$. A system with three-cell frequency reuse using the 10 element array on the uplink is simulated. This system can support 0.3

users/cell/channel with a 5 - 6 dB improvement in C/I compared with a similar system using a sector antenna and supporting only 0.1 users/cell/channel [5].

W. C. Y. Lee, on the title "Applying the Intelligent Cell Concept to PCS," works on reducing the required carrier to interference ratio (as measured with an omnidirectional antenna) using adaptive antennas. This allows the system to have fewer cells in a cluster and increases spectral efficiency [6].

Somnath Patra et al [7] on the title "Power pattern synthesis of smart antenna array using different adaptive algorithms," a smart or adaptive antenna array system is optimized using LMS, RLS and SMI. The performance of these three algorithms based on the response towards co-channel interference, the rate of convergence and complexity is compared. And the superiority of RLS algorithm is proved by the proposed approach.

J. Jin, H. L. Wang, W. M. Zhu, and Y. Z. Liu, with title "Array Patterns Synthesizing Using Genetic Algorithm" a planar array antenna with arbitrary geometry synthesis technique based on genetic algorithm used this approach avoids coding/decoding and directly works with complex numbers to simplify computing programming and to speed up computation. Simulation results show that this method is capable of synthesizing arrays whose elements are located on irregular grids, and generates quite complex shapes and can realize good sidelobe suppression at the same time. This approach is capable of synthesizing quite complex shapes of 3D patterns for main lobe and can realize good side lobe suppression at the same time. The method has been proved to be useful for the synthesis of large array antennas whose elements are located on irregular grids [8].

T. Yuan, N. Yuan, L.-W. Li, and M.-S. Leong with title "Design and Analysis of Phased Antenna Array with Low Sidelobe by Fast Algorithm" high performance phased antenna array is designed. Compared with the traditional ones, this antenna array has a lower sidelobe characteristic of down to −16 dB. At different scanning angles, the comparison between calculated and measured results of S-parameters and E- and H-plane antenna patterns is made and a very good agreement is found [9].

Ch. Santhi rani, Dr. P.V Subbaiah and Dr.K. Chennakesava reddy in [10] with title "Smart Antenna Algorithms for WCDMA Mobile Communication Systems," discussed about adaptive

beamforming algorithms like Direct Matrix Inversion algorithm (DMI) and Recursive Least Square algorithms (RLS) used in smart antennas. The result obtained from the simulations showed that the DMI had poor convergence compared to RLS, and the RLS algorithm is the most efficient algorithm.

In [11] with title "LMS and RLS Algorithms for Smart Antennas in a W-CDMA Mobile Communication Environment" discussed about adaptive beamforming algorithms like Least Mean Square (LMS) and Recursive Least Squares (RLS) algorithms used in smart antennas. Simulation results were provided to understand the convergence, stability, and the method of the adaptation of the algorithm. The results obtained from the simulations showed that the LMS had poor convergence compared to RLS, and the RLS algorithm is the most efficient and LMS is the slowest.

Seifu G. [12] in his work, adaptive beamforming algorithms for smart antenna system are investigated. Particularly the effect of angle separation on the performance of adaptive array system such as: side lobe level, bore sight and nulling are presented. From his simulation results he observed that, increasing spacing between array elements for small angle of separation system performance enhances at the cost of grating lobes. The other observation in his simulation is that increasing the number of array increase the system performance for all angle of separation.

All of the above researches contribute for the analysis of smart antenna system in terms of different performance parameters. This thesis incorporates comparative analysis of SLL of non-blind adaptive algorithms for smart antenna mobile communication system.

1.3 Statement of the Problem

As an aim of providing good Quality of Service (QoS) for customers, it is desired to minimize interference and increase the data rate in the direction of the desired user. One of the means for achieving good QoS is using smart antenna system. Smart antennas use smart signal processing algorithm and they are capable of identifying the signal structure such as Direction of Arrival (DOA) and this is further used to calculate beamforming vectors. These beamforming vectors have the ability to track and locate the antenna beam on the mobile device. The smart antenna performs

these functions of DOA and beamforming using different types of adaptive beamforming algorithms. Like other antenna types, the smart antenna produces radiation lobes and one of these lobes is the sidelobe which is a radiation lobe in any direction other than the intended lobe.

Since *a sidelobe* is a radiation lobe in any direction other than the intended lobe, reducing its level will reduce radiation in undesired direction, interferences from other direction and increases Signal-to-Interference-plus-Noise Ratio. But when the sidelobe level of the antenna pattern becomes large there is wastage of energy and more interference creation in the system and this in turn degrades the performance of the communication system. One of the solution for overcoming this performance degradation is using a smart antenna with an algorithm that produces lower SLL. So for increasing the smart antenna capacity and reducing its interference level, it is required to know which of the non-blind adaptive algorithms among the LMS, SMI and RLS produces lower SLL. For that matter, this thesis is centered to the comparative analysis of these non-blind adaptive algorithms on the basis of sidelobe level.

1.4 Objectives of the Thesis

1.4.1 General Objective

- To investigate the comparative analysis of non-blind adaptive algorithms in terms of sidelobe level for adaptive smart antenna in cellular mobile communication system.

1.4.2 Specific Objective

- To investigate the beamforming status of LMS, SMI and RLS algorithms in terms sidelobe level for adaptive smart antenna system.
- To investigate the effect of number of elements of an array and inter-element spacing on sidelobe level of smart antenna.

1.5 Methodology

The methods to be employed to achieve the objectives of the thesis are:

- **Literature Review**: includes reading journals, books, articles, simulation tools and other resources related to the topic.

- **System Modeling:** involves the formulation of smart antenna systems, adaptive algorithms and signal parameters that are used in this work.
- **Simulation:** involves simulating the modeled communication system using beamforming algorithms and MATLAB.
- **Analysis and Interpretation of the results:** the results obtained from the simulation results analyzed and compared based on sidelobe level of the array factor pattern.

1.6 Assumptions taken in this thesis

It is known that array geometry and element spacing are important factors in the design of an antenna array. If the elements are more than λ/2 apart, then the grating lobes appear which degrades the array performances.

Mutual coupling is an effect that limits the inter-element spacing of an array. If the elements are spaced closely (typically less than λ/2), the coupling effects will be larger and generally tend to decrease with increase in the spacing. Therefore, the elements have to be far enough to avoid mutual coupling and the spacing has to be smaller than λ/2 to avoid grating lobes. For all practical purposes, a spacing of λ/2 is preferred [13]. An antenna array can be arranged in any arbitrary fashion, but the most preferred geometries are linear and circular geometries. Linear geometry is simpler to implement than the circular geometry. Linear array with uniformly spaced sensors is the most commonly used structure. This type of array, Uniform Linear Array (ULA) with identical distortionless elements, is used for this thesis work. And it is considered that the reference (first) element is situated at the origin so that the signal as it travels across the array undergoes a phase shift which is described in [13] for uniform circular array. The relation holds for a narrowband signal whose modulated bandwidth is much less than the carrier frequency travelling through a homogenous medium. The narrowband assumption allows us to assume that the only difference between the signal present at different elements of the array is the phase shift induced by the extra distance traveled (pure time delay) and is not significantly affected by the modulation during this time.

Generally, the assumptions taken in this thesis can be summarized as:

- The array consists of identical distortion free element

- The first element is situated at the origin
- Equal inter-element spacing for the arrays (d)
- The signals are narrow bands
- The signals are uncorrelated
- Homogenous medium
- The effect of the propagation from a source to an element is a pure time delay.
- Considering M directional sources

1.7 Significance of the Study

The use of smart antenna in wireless mobile communication is an essential component for increasing capacity of the communication system through the reduction of sidelobe level using different algorithms. This thesis compares non-blind adaptive algorithms in terms of sidelobe level of adaptive smart antenna. It will have its own contribution on use of adaptive beamforming techniques for improving capacity and reducing interference to maximize the desired signal reception. The completed research can also be used as a guideline for future related works on the area.

The thesis may also have its own part of significance for smart antenna manufacturers in designing adaptive antenna systems for network deployment. In general, the research will have important significance for whom requiring reference related to non-blind adaptive algorithms of smart antenna system.

1.8 Organization of the thesis

The next chapters of this thesis are organized as follows. Chapter 2 describes about the fundamentals of smart antenna. Some introductory ideas about smart antenna and the criteria for optimum beamforming are presented in this chapter. Chapter 3 is about adaptive beamforming algorithms. Under this chapter, the non-blind adaptive algorithms that are used for this thesis are fully described.

In Chapter 4 simulation results of non-blind adaptive algorithms and plot analysis based on sidelobe level of three algorithms is presented. Finally, in Chapter 5, conclusion based on the simulation results and future work recommendations are presented.

Chapter 2: Fundamentals of Smart Antenna

2.1 Introduction

Traditional array antennas, where the main beam is steered to directions of interest, are called *phased arrays, beamsteered arrays*, or *scanned arrays*. The beam is steered via phase shifters and in the past these phase shifters were often implemented at RF frequencies. This general approach to phase shifting has been referred to as electronic beam steering because of the attempt to change the phase of the current directly at each antenna element. Modern beamsteered array antennas, where the pattern is shaped according to certain optimum criteria, are called *smart antennas*. Smart antennas have alternatively been called *digital beamformed* (DBF) arrays or *adaptive arrays* (when adaptive algorithms are employed). The term *smart* implies the use of signal processing in order to shape the beam pattern according to certain conditions. For an array to be *smart* implies sophistication beyond merely steering the beam to a direction of interest. Smart essentially means computer control of the antenna performance [14].

Radiation pattern of smart antenna are controlled via algorithms based up on certain criteria. These criteria could be maximizing the signal-to-interference ratio (SIR), minimizing the variance, minimizing the Mean Square Error (MSE), steering toward a signal of interest, and nulling the unwanted interfering signals. The implementation of these algorithms can be performed electronically through analog devices but it is generally more easily performed using digital signal processing.

In the following sections of this chapter, the smart antenna basic characteristics, optimum beamforming criteria and DOA methods are introduced.

2.2 Smart Antenna

Adaptive beamforming smart antennas have numerous important benefits in wireless applications as well as in sensors such as radar. In the case of mobile wireless applications, smart antennas can provide higher system capacities by directing narrow beams toward the users of interest, while nulling other users not of interest. This allows for higher signal-to-interference

ratios, lower power levels, and permits greater frequency reuse within the same cell. This concept is called space division multiple access (SDMA).

Other benefits of smart antenna include: -

- Deleterious effects of multipath can be mitigated,
- Higher data rate by reducing simultaneously co-channel interference and multipath fading,
- Enhance direction finding techniques by accurately finding direction of arrival of signals,
- Direct the array main beam toward signals of interest even when no reference signal or training sequence is available. This capability is called blind adaptive beam forming,
- Sidelobe canceling or null steering and
- MIMO compatibility in both communications and radar.

In terms of function, smart antenna performs beamforming and estimation of direction of arrival of signals. The beamforming function is intended to create the radiation pattern of the antenna arrays by adding constructively the phase of the signals in the direction of desired users and nulling the pattern of undesired users(interferers). In this function of smart antenna both the amplitude and phase of each antenna element is controlled. The control of amplitude and phase of the elements is used to adjust sidelobe levels and steer nulls. The Direction of Arrival (DOA) can be achieved using different methods of algorithms. The beamforming and direction of arrival functions are discussed in the following sections.

2.3 Smart Antenna Beamforming Function

A Beamformer is an array of sensors which can do spatial filtering. It does spatial filtering in the sense that it separates two signals with overlapping frequency content originating from different directions [14]. Spatially propagating signals encounter the presence of interfering signals and noise signals. If the desired signal and the interferers occupy the same temporal frequency band, then temporal filtering cannot be used to separate the signal from the interferers. The optimum beamforming algorithm works if the correlation matrix (R) between the signals induced in each array elements and the correlation between the reference and the induced signal (r) available and the direction of arrival (signal environment) is not changing. However, in practice these may not

appear always, so the task of adaptive beamforming is estimating the optimal weight for rapidly changing channel state and DOA. Adaptive beamforming algorithms iteratively approximate these optimum weights. However, the desired and the interfering signals generally originate from different spatial locations. This spatial separation can be exploited to separate the signals from the interference using a beam former. The output of each sensor is properly filtered and the filtered outputs of all the sensors are added up. Typically, a beamformer linearly combines the spatially sampled waveform from each sensor. Beamforming is the process by which the information, obtained from the signals incident on an antenna array, are used to generate an optimum pattern which maximizes the radiated power towards the intended users and minimizes it, in the form of radiation nulls, towards interferers [15]. The objective of beamforming is to separate the desired signal from interfering signals, given that they have the same frequencies but different spatial locations. Interfering signals can be the delayed version of the desired one. A beamformer consists of an array of sensors in a particular configuration as shown in figure below.

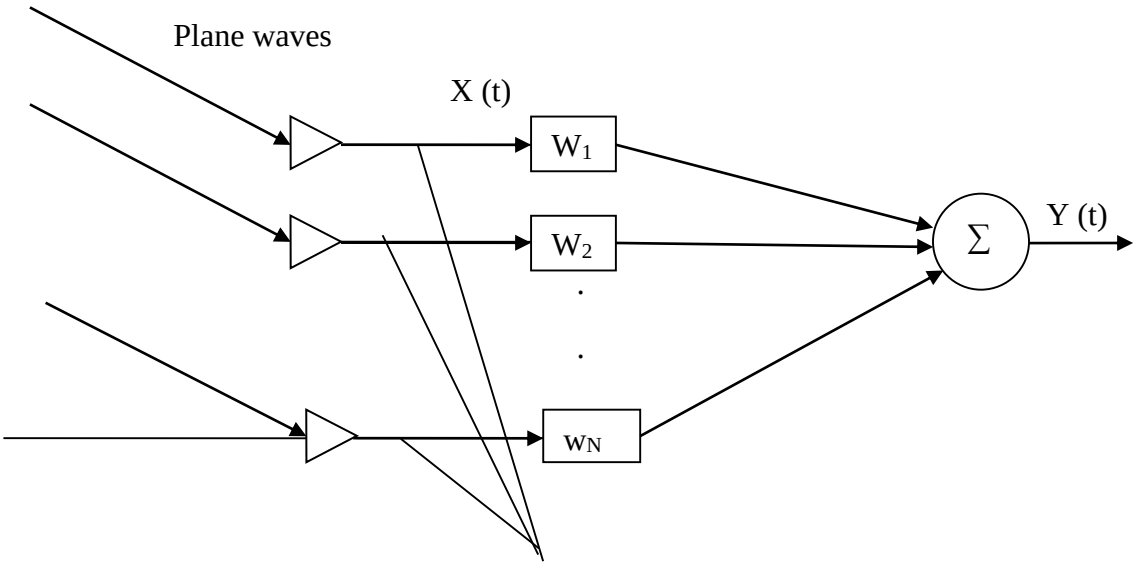

Figure 2.1: General beamformer system of smart antenna [12]

For the induced signals X (t) and weight W, the output signal is given by:

$$Y(t) = W^{H}.X(t) \quad (2.1)$$

but signal induced on the i^{th} element due to the k^{th} source can be expressed as:

$$\mathbf{X}_i(t) = M_k(t) e^{j2\pi f_0(t+\tau(\theta_k))} \quad (2.2)$$

Where $M_k(t)$ =complex modulating function, for narrow band signals it can be expressed as:

$$M_k(t) = M_k(t+\tau) \quad (2.3)$$

The signal induced due to all M directional sources and additional propagation environmental noises $n_i(t)$ on the i^{th} element is given by

$$X_i(t) = \sum_{k=1}^{M} M_k(t)\, e^{j2\pi f_0(t+\tau(\theta_k))} + n_i(t) \quad (2.4)$$

Using vector notation, the signal induced on all elements, the weights and noise can be represented as:

$$X(t) = [x_1(t), x_2(t) \ldots . x_N(t)]^T \quad (2.5)$$

$$W = [w_1, w_2, \ldots w_N] \quad (2.6)$$

$$n(t) = [n_1(t), n_2(t). \ . \ . \ n_N(t)]^T \quad (2.7)$$

By defining N-dimensional complex vector of steering vector containing the response of all elements of the array to narrow band sources as S_k which is associated with the k^{th} source for the array of identical elements as:

$$\mathbf{S}_k = [e^{2\pi f_0 \tau_1(\theta_k)}, e^{2\pi f_0 \tau_2(\theta_k)} . \ . \ . \ e^{2\pi f_0 \tau_N(\theta_k)}] \quad (2.8)$$

Substituting S_k in the exponential term and vector notations, the induced signal becomes:

$$X(t) = \sum_{k=1}^{M} M_K(t)\, S_K + n(t) \quad (2.9)$$

Using this equation of induced signal, the output of smart antenna becomes:

$$Y(t) = \sum_{k=1}^{M} M_K(t) W^H S_k + W^H n(t) \quad (2.10)$$

Where W^H is the complex weight vector. The weights of the array system determine system performance. The selection process of these weights depends on the application and leads to various types of beamforming schemes. The first term in this equation shows all directional sources

contribution and the second term is related to the random noise contribution to the array output [12].

2.4 Criteria for optimal beamforming

The weight on each antenna element in adaptive smart antenna is adjusted based on the statistics of the array data. In general, the adaptive smart antenna adjusts the weight vector such that it places nulls in the direction of interfering signals in an attempt to maximize the SNR at the beam former output. Adaptive algorithms are typically employed to determine the weights even the statistics of the array data is not known. Most adaptive beamforming algorithms involve iterative process to adjust the weights until a certain performance criterion is met. The weights w_n can be chosen to meet any specific criteria. Generally, the criterion is to minimize the sidelobes or possibly to place nulls at certain angles [14].

The most common performance criteria are the Minimum Mean-Squared Error (MMSE) and Maximum Signal-to-Interference-plus-Noise Ratio (MSINR). An antenna is optimal when the weight of each antenna element is adjusted to achieve optimal performance of an array system in some sense.

2.4.1 Minimum Mean-Square Error

In this criteria the shape of the desired received signal waveform is known by the receiver and complex weights are adjusted to minimize the mean-square error between the beamformer output and the expected signal waveform.
The following figure shows a smart antenna configuration with the assumption of uniform distance between antenna elements and uncorrelated narrow band induced signals with no coupling.

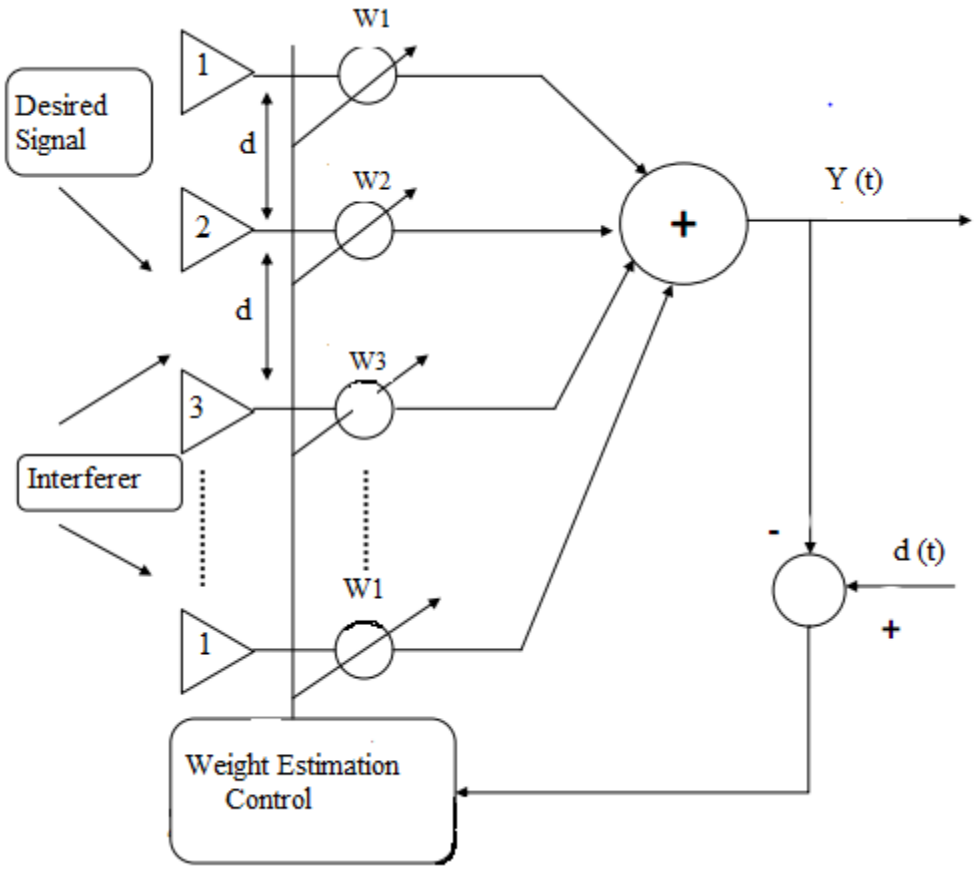

Figure 2.2: Smart antenna with weight consideration [12]

Considering the above figure, using the mean square error, the error signal between the desired signal and the array output is:

$$e(t) = d(t) - Y(t) \tag{2.11}$$

But from equation (2.1) the array output is $Y(t) = W^H . X(t)$

$$e(t) = d(t) - W^H . X(t) \tag{2.12}$$

This implies the mean square error becomes

$$= |d(t) - W^H . X(t)|^2 \tag{2.13}$$

By expanding the above we get:

$$|e(t)|^2 = |d(t)|^2 - 2d(t)\, W^H . X(t) + W^H . X(t) . X(t)^H . W \tag{2.14}$$

Taking the expected value of both sides and simplifying the expression we get

$$E[|e(t)|^2] = E[|d(t)|^2 - 2\times d(t)\, W^H.\, X(t) + W^H.X(t).X(t)^H.W] \quad (2.15)$$

$$E[|e(t)|^2] = E[|d(t)|^2] - 2W^H r + W^H R_{xx} W \quad (2.16)$$

Where r = E [d*.X] is the correlation between the reference and the induced signal.

$R_{xx} = E[X . X^H]$ is the correlation matrix between the signals induced in each array elements.
Equation (2.16) is sometimes called cost function or performance surface. Since the optimum weights provide the minimum MSE, the extremum is the minimum of this function. The minimum value can be found by taking the gradient of the MSE with respect to the weight vectors and equating it to zero. Thus from Wiener-Hopf equation given as

$$\nabla_w (E[|e|^2]) = 2R_{xx}W - 2r = 0 \quad (2.17)$$

Rearranging yields:

$$\mathbf{W}_{opt} = R_{xx}^{-1} r \quad (2.18)$$

2.4.2 Maximum Signal-to-Interference-plus-Noise Ratio

Considering the previous figure, where signals from each element are multiplied by a complex weight and summed to form the array output and in this performance criterion the weights should be adjusted to directly maximize the output Signal-to-Interference-Plus-Noise Ratio (SINR) where the receiver can estimate the strengths of the desired signal and of an interfering signal.
The output power of the array at any time t as expressed in [14] is given by:

$$P(t) = |Y(t)|^2 \quad (2.19)$$

$$P(t) = Y(t)\, Y(t)^* \quad (2.20)$$

Substituting for Y (t) we get:

$$P(t) = W^H X(t)\, X(t)^H W \quad (2.21)$$

By assuming **X (t)** as a zero mean stationary processes, the mean output power of the array system is obtained by taking the expectation over **X (t)**

$$P(w) = E[|W^H X(t)|^2] \quad (2.22)$$

$$= E[\{W^H X(t)\}\, \{W^H X(t)\}^*]$$

$$= W^H E[X(t)\, X(t)^*]\, W$$

$$= W^H R W \tag{2.23}$$

Let $X_S(t)$, $X_I(t)$ and $n(t)$, denote the signal vector due to the desired signal source, unwanted interference, and random noise respectively with the assumption of existence of unwanted interference and a random noise signals with the desired signal. The output components of these signals are obtained by taking the inner product of the weight vector with $X_S(t)$, $X_I(t)$ and $n(t)$ as follows:

$$Y_S(t) = W^H X_S(t) \tag{2.24}$$

$$Y_I(t) = W^H X_I(t) \tag{2.25}$$

$$Y_n(t) = W^H n(t) \tag{2.26}$$

By defining the array correlation matrices due to the signal source, unwanted interference, and random noise, respectively, as

$$R_S(t) = E[X_S(t)\, X_S^H(t)] \tag{2.27}$$

$$R_I(t) = E[X_I(t)\, X_I^H(t)] \tag{2.28}$$

$$R_n(t) = E[n(t)\, n^H(t)] \tag{2.29}$$

The sum of these three matrices becomes as R

$$R = R_S + R_I + R_n \tag{2.30}$$

Denoting P_S, P_I and P_n as the mean output power due to the signal source, unwanted interference, and random noise, respectively.

$$P_S = W^H R_S W \tag{2.31}$$

$$P_I = W^H R_I W \tag{2.32}$$

$$P_n = W^H R_n W \tag{2.33}$$

Let $\mathbf{P_N}$ denote the mean power at the output of the array contributed by random noise and unwanted interference, that is,

$$P_N = P_I + P_n \tag{2.34}$$

By substituting the value of P_I and P_n we get

$$P_N = W^H R_I W + W^H R_n W$$

$$= W^H (R_I + R_n) W \quad (2.35)$$

And let $\mathbf{R_N}$ denote the noise array correlation matrix, that is,

$$R_N = R_I + R_n \quad (2.36)$$

Then P_N, the mean noise power at the output of the system can be expressed in terms of weight vector and $\mathbf{R_N}$ as

$$P_N = W^H R_N W \quad (2.37)$$

Let the output Signal to Interference plus Noise Ratio (SINR), be defined as the ratio of the mean output signal power to the mean output noise power at the output of the array system, that is,

$$\text{SINR} = \frac{PS}{PN} \quad (2.38)$$

Substituting the value of corresponding terms as in [11] we get

$$\text{SINR} = \frac{W^H R_S W}{W^H R_N W} \quad (2.39)$$

To maximize the output SINR, we take the derivative of equation with respect to W and set it to zero, which gives the following result:

$$R_S W = \frac{\mathbf{W^H R_S W}}{\mathbf{W^H R_N W}} R_N W \quad (2.40)$$

Direction of Arrival Estimation

In adaptive smart antenna system, there are two methods of estimation of direction of arrival signal. Spectral Estimation Methods and Eigen structure methods. Minimum Variance Distortionless Response Estimator, Bartlett Method, Linear Prediction Method, Maximum Likelihood Method are some of spectral estimation methods and music methods, sprit method, CLOSEST Method, ESPRIT Method are included in Eigen structure methods.

2.5 Methods of Spectral Estimation

Spectral Estimation methods estimates the DOA of the incoming signal by computing mean power received by an antenna array that is also known as the spatial spectrum $p(\theta)$, as a function of direction of arrival (θ) and then determining the local maxima of this computed spatial spectrum. Among some of these methods are:

2.5.1 Linear Prediction Method

This is type of prediction method estimates the output of one sensor using linear combinations of the remaining sensor outputs and minimizes the mean square prediction error, that is, the error between the estimate and the actual output [16]. Implying that, it obtains the array weights by minimizing the mean output power of the array subject to the constraint that the weight on the selected sensor is unity.

2.5.2 Minimum Variance Distortionless Response Estimator

The minimum variance distortionless response estimator (MVDR) is the Maximum Likelihood Method (MLM) of spectrum estimation which finds the Maximum Likelihood (ML) estimate of the power arriving from a point source in direction θ assuming that all other sources are interference [16].

2.5.3 Maximum Likelihood Method

The MLM estimates the DOAs from a given set of array samples by maximizing the log likelihood function. The Likelihood function is the joint probability density function of the sampled data given the DOAs and viewed as a function of the desired variables, which are the DOAs in this case. The method searches for those directions that maximize the log of this function. The ML criterion signifies that plane waves from these directions are most likely to cause the given samples to occur maximization of the log-likelihood function is a nonlinear optimization problem, and in the absence of a closed-form solution requires iterative schemes. [16]. The MLM provides superior performance [14] compared to other methods particularly when SNR is small, the number of samples is small, or the sources are correlated and thus is of practical interest.

2.6 Eigen Structure Methods

These methods rely on the following properties of the array correlation matrix:

- The space spanned by its eigenvectors may be partitioned in two subspaces, namely the signal subspace and the noise subspace; and
- The steering vectors corresponding to the directional sources are orthogonal to the noise subspace.

As the noise subspace is orthogonal to the signal subspace, these steering vectors are contained in the signal subspace. It should be noted that the noise subspace is spanned by the eigenvectors associated with the smaller eigenvalues of the correlation matrix, and the signal subspace is spanned by the eigenvectors associated with its larger eigenvalues. Eigen structure methods may also be used for finding DOAs when the background noise is not white [16].

2.6.1 MUSIC Methods

The multiple signal classification (MUSIC) method is a relatively simple and efficient Eigen structure variant of DOA estimation methods. It is perhaps the most studied method in its class and has many variations. Like Spectral MUSIC, Root-MUSIC, Constrained MUSIC and Beam Space MUSIC are some of its class.

Spectral MUSIC

In its standard form, also known as spectral MUSIC, the method estimates the noise subspace from available samples. This can be done either by eigenvalue decomposition of the estimated array correlation matrix or singular value decomposition of the data matrix with its N columns being the N array signal vector samples, also known as snapshots [17]. The latter is preferred for numerical reasons.

Once the noise subspace has been estimated, a search for M directions is made by looking for steering vectors that are as orthogonal to the noise subspace as possible.

Root-MUSIC

For a uniformly spaced linear array (ULA), the MUSIC spectra can be expressed such that the search for DOA can be made by finding the roots of a polynomial. In this case, the method is known as root-MUSIC. Thus, root-MUSIC is applicable when a ULA is used and solves the

polynomial rooting problem in contrast to spectral MUSIC's identification and localization of spectral peaks. Root-MUSIC has better performance than spectral MUSIC [17].

Constrained MUSIC

This method incorporates the known source to improve estimates of the unknown source direction. The situation arises when some of the source directions are already known. The method removes signal components induced by these known sources from the data matrix and then uses the modified data matrix for DOA estimation. Estimation is achieved by projecting the data matrix onto a space orthogonal complement to a space spanned by the steering vectors associated with known source directions. A matrix operation, the process reduces the signal subspace dimension by a number equal to the known sources and improves estimate quality, particularly when known sources are strong or correlated with unknown sources.

Beam Space MUSIC

The MUSIC algorithms discussed so far process the snapshots received from sensor elements without any preprocessing, such as forming beams, and thus may be thought of as element space algorithms, which contrasts with the beam space MUSIC algorithm in which the array data are passed through a beamforming processor before applying MUSIC or any other DOA estimation algorithms. The beamforming processor output may be thought of as a set of beams; thus, the processing using these data is normally referred to as beam space processing. The DOA estimation in beam space has a number of advantages such as reduced computation, improved resolution, reduced sensitivity to system errors, reduced resolution threshold, reduced bias in the estimate, and so on. These advantages arise from the fact that a beamformer is used to form a number of beams that are less than the number of elements in the array; consequently, less data to process DOA estimation are necessary.

2.6.2 CLOSEST Method

The CLOSEST method is useful for locating sources in a selected sector. Contrary to beam space methods, which work by first forming beams in selected directions, CLOSEST operates in the element space and in that sense it is an alternative to beam space MUSIC. In a way, it is a generalization of the minimum-norm method [14]. It searches for array weights in the noise

subspace that are close to the steering vectors corresponding to DOAs in the sector under consideration, and thus its name. Depending on the definition of closeness, it leads to various schemes. A method referred to as FINE (First Principal Vector) selects an array weight vector by minimizing the angle between the selected vector and the subspace spanned by the steering vectors corresponding to DOAs in the selected sector.

2.6.3 ESPRIT Method

Estimation of signal parameters via rotational invariance techniques is a computationally efficient and robust method of DOA estimation. It uses two identical arrays in the sense that array elements need to form matched pairs with an identical displacement vector, that is, the second element of each pair ought to be displaced by the same distance and in the same direction relative to the first element.

Chapter 3: Adaptive Antenna Algorithms

3.1 Introduction

In adaptive beamforming, the target is to adapt the beam by adjusting the amplitudes and phases of signals such that an enviable pattern is formed. Adaptive beam forming algorithms are classified into two groups, known as non-blind adaptive algorithms and blind adaptive algorithms.

As first part of this chapter, brief description of blind adaptive algorithms is presented. And the next part of this chapter is about the non-blind algorithms (LMS, RLS and SMI) which are algorithms used for this thesis work.

3.2 Blind Algorithms

Unlike training-based algorithms, blind algorithm do not require training signals to adapt their weights. Therefore, these algorithms save transmission bandwidth. Blind algorithms can be classified as property restoral algorithms, channel estimation algorithms, and dispread and respread algorithms. Property restoral algorithms restore certain properties of the desired signal and hence enhance the SINR. The property that is being restored may be the modulus or the spectral coherence. Blind property restoral algorithms can be classified as Constant Modulus (CM) algorithm, Spectral self-Coherence Restoral (SCORE) algorithms, and decision directed (DD) algorithms. Channel estimation techniques [18] use the knowledge of the special code properties of the spread spectrum signals to obtain estimates of the channel parameters. These techniques first estimate the channel parameters and then use the channel estimates to form beams in the direction of the desired signals. These techniques are applicable only for CDMA signals.

Despread-respread techniques for CDMA belong to the family of demod-remod techniques, which is common in FM interference rejection. A despread-respread technique works on the principle of despreading the signal at the output of the i^{th} user and then making a bit decision. The error between the respread data and the output of the array is minimized using a least-squares or a steepest descent approach. The assumption behind the despread-respread based adaptation is that the

synchronization has been achieved prior to beamforming, since despreading requires synchronization.

3.3 Training based (Non-Blind) Algorithms

Non-blind algorithms use a training signal d (n) to update its complex weight vectors and they are employed to minimize mean square error. LMS, RLS, SMI and other types of algorithms are categorized as non-blind algorithms. The processor in the adaptive array has a pre-stored training signal and the array adapts its weights when the training signal is transmitted by the transmitter. This technique requires synchronization. These algorithms work very well, but the only cost paid is the excess transmission time or wastage of bandwidth.

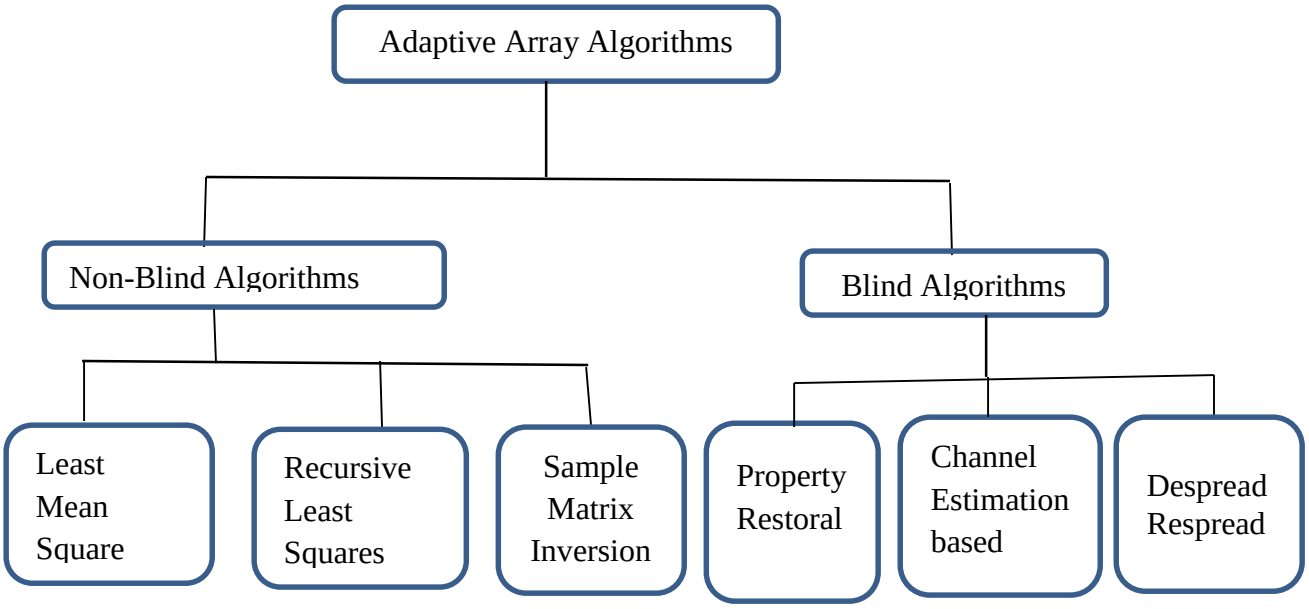

Figure 3.1: Classification of adaptive algorithms [12]

3.3.1 Least-Mean-Square Algorithm

The Least Mean Square (LMS) algorithm, introduced by Widrow and Hoff in 1959 is an adaptive algorithm, which uses a gradient-based method of steepest decent.

The least-mean-square (LMS) is a search algorithm in which a simplification of the gradient vector computation is made possible by appropriately modifying the objective function. The LMS

algorithm, as well as others related to it, is widely used in various applications of adaptive filtering due to its computational simplicity [14].

The LMS algorithm is by far the most widely used algorithm in adaptive filtering for several reasons. The main features that attracted the use of the LMS algorithm are low computational complexity, proof of convergence in stationary environment, unbiased convergence in the mean to the Wiener solution, and stable behavior when implemented with finite-precision arithmetic.

The optimum Wiener solution $\mathbf{W_{opt}=R_{xx}^{-1}r}$ requires the calculation of the inverse of the correlation matrix ***R*** and this results in a high computational complexity. The Least mean square algorithm is a gradient based quadratic approach. Gradient algorithms assume an established quadratic performance surface which is a function of the array weights, the performance surface *J (W)* is the shape of an elliptic parabola having one minimum [19]. One of the best ways to establish the minimum is through gradient method. We can establish the performance surface (cost function) by again finding the MSE. Therefore, the spatial filtering problem involves estimation of signal from received signal (i.e. the array output) by minimizing error between the reference signal *d (t)* (which closely matches or has some extent of correlation with the desired signal estimate) and the beamformer output ***y (t)*** equal to $\mathbf{W^H}$ ***x (t).*** This is a classical wiener filtering problem for which solution can be iteratively found using the LMS algorithm.

The induced signal x (t) received by multiple antenna elements is multiplied with the coefficients in a weight vector w (series of amplitude and phase coefficients) which adjusted the phase and the amplitude of the incoming signal accordingly. The weighted signal is summed up, resulted in the array output *y (t)*. An adaptive algorithm is then employed to minimize the error *e(t)* between a desired signal *d(t)* and the array output *y (t)* given by linear combination of the data at the k sensors.

The Least-Mean-Square (LMS) Algorithm avoids matrix inverse operation by using the instantaneous gradient vector ***J (w)*** to update the weight vector. The steepest descent iterative approximation is given as [20]

Using the equation:

$$W(k+1) = W(k) - \frac{1}{2}\mu \nabla_W J(W(k)) \qquad (3.1)$$

As indicated above μ is the convergence factor which controls the speed of convergence and its value is usually between 0 and 1 and ∇_w is the gradient of the performance surface. The direction of steepest

descent is in the opposite direction as the gradient vector. An exact measurement of the instantaneous gradient vector is not possible since this would require a prior knowledge of both the correlation matrix ***R*** and the cross-correlation vector ***r***. Instead, an instantaneous estimate of the gradient vector is used which is given by

$$\nabla_W(J\ (W\ (k))) = -2r\ (k) + 2R\ (k)\ W\ (k) \tag{3.2}$$

Where

$$R_{xx}\ (k) = E\{X\ (k).X^H\ (k)\} \tag{3.3}$$

$$r\ (k) = \{d^*(k).\ X\ (k)\} \tag{3.4}$$

If these values are substituted in the gradient of performance surface, we can get the LMS solution as:

$$W\ (k+1) = W\ (k)-\mu\ [R_{xx}W - r]$$

$$=W\ (k) + \mu e^*(k).X\ (k) \tag{3.5}$$

Where

$$e\ (k) = d\ (k) - W^H.X\ (k) \text{ is the error signal}$$

The LMS algorithm is a member of stochastic gradient algorithms since the instantaneous estimate of the gradient vector is a random vector that depends on the input vector x (k). It requires only 2*M* complex multiplications per iteration, where *M* is the number of weights used in the adaptive array [21].

The LMS algorithm is initiated with an arbitrary value W (0) for the weight vector at k = 0. The successive corrections of the weight vector eventually lead to the minimum value of the mean squared error. The step-size parameter or the convergence factor $\boldsymbol{\mu}$ is the basis for the convergence speed of the LMS algorithm. The LMS algorithm initiated with some arbitrary value for the weight vector is seen to converge and stay stable for:

$$0 < \mu < \frac{1}{\lambda_{max}}$$

Where λ_{max} is the largest Eigen value of the correlation matrix R. If μ is chosen to be very small, the algorithm converges very slowly. A large value of μ may lead to a faster convergence but there may a stability problem [22].

The following figure shows the flow chart of LMS algorithm. For this case the array parameters such as: spacing and number of arrays are set before the estimation of angle of arrival.

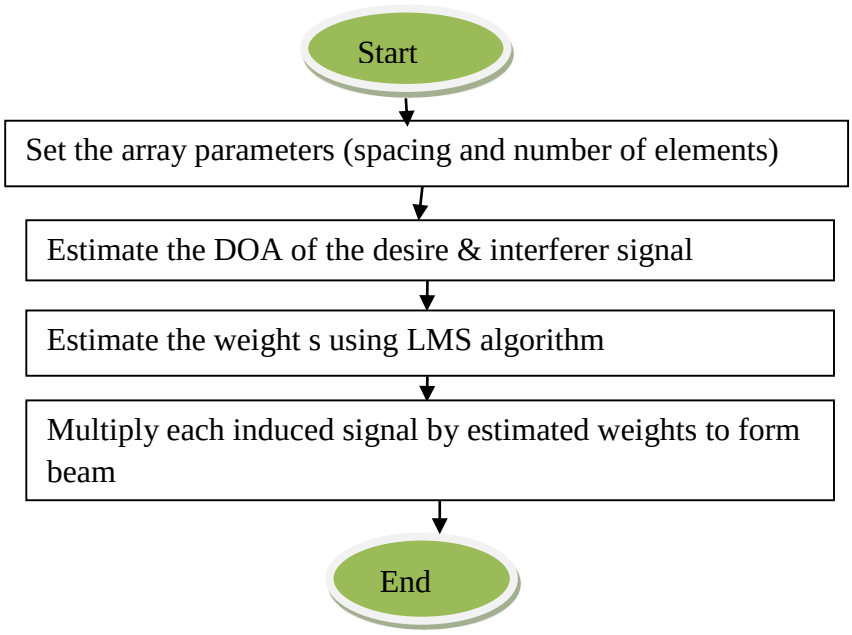

Figure 3.2: Flow chart of LMS adaptive beamforming algorithm

3.3.2 Sample Matrix Inversion Algorithm

The Sample Matrix Inversion (SMI) is also called as Direct Matrix Inversion (DMI) algorithm. Sample matrix is a time average estimate of the array correlation matrix using k-time samples. If the random process is ergodic in the correlation, the time average estimate will equal the actual correlation matrix. The idea of sample matrix inversion algorithm is to estimate the correlation matrix R and the cross-correlation vector r based on the samples of the array sensor input in an observation interval so that the speed of convergence is improved.

From the optimum Wiener solution

$$\mathbf{W} = \mathbf{R_{xx}^{-1}}\,\mathbf{r} \tag{3.6}$$

Where

$$Rxx = E\,[X\,.X^{H}]$$

$$r = E\,[d^{*}.X]$$

From this we can estimate the correlation matrix by calculating the time average such that

$$Rxx = \frac{1}{k}\sum_{k=1}^{K} X(k)\,X(k)^{H} \tag{3.7}$$

Where K is the observational interval.

The correlation vector r can also be estimated as

$$\mathrm{r} = \frac{1}{k}\sum_{k=1}^{K} d(k)^{*}\mathrm{X}\ (\mathrm{k}) \tag{3.8}$$

The K-length block of data is called a block adaptive approach. It uses the weights block-by-block.

It is easy in MATLAB [14] to calculate the array correlation matrix and the correlation vector by the following procedure. Define the matrix $\bar{X}_{\mathrm{K}}(\mathrm{k})$ as the kth block of $\bar{x}$ vectors ranging over K-data snapshots. Thus

$$\bar{X}_K(k) = \begin{bmatrix} x_1(1+kK) & x_1(2+kK) & \dots & x_1(K+kK) \\ \vdots & \vdots & & \vdots \\ x_M(1+kK) & x_M(2+kK) & \dots & x_M(K+kK) \end{bmatrix} \tag{3.9}$$

Where k is the block number and K is the block length. Thus, the estimate of the array correlation matrix is given by:

$$\hat{R}\mathrm{xx(k)} = \frac{1}{K}\bar{X}_K(k)\bar{X}^H{}_K(k) \tag{3.10}$$

In addition, the desired signal vector can be defined by:

$$\bar{d}(k) = [\mathrm{d(1+kK)} \quad \mathrm{d(2+kK)} \quad \cdots \quad \mathrm{d(K+kK)}] \tag{3.11}$$

Thus the estimate of the correlation vector is given by

$$\hat{r}(\mathrm{k}) = \frac{1}{K}\bar{d}^{*}(k)\bar{X}_K(k) \tag{3.12}$$

The SMI weights can then be calculated for the k^{th} block of length K as

$$\bar{w}_{SMI} = \hat{R}_{xx}{}^{-1}(k)\,\hat{r}(\mathrm{k}) = [X(k)X^H(k)]^{-1}\mathrm{d}^{*}(\mathrm{k})\ \mathrm{X}\ (\mathrm{k}) \tag{3.13}$$

3.3.3 Recursive Least Square Algorithm

Even though the SMI method is faster than the LMS algorithm, the computational burden and potential singularities can cause problems. However, we can recursively calculate the required correlation matrix (R) and the required correlation vector (r). As we have seen above for the case of SMI, there is division of sum terms by the block length K to calculate R and r. The block length K vanishes in calculating the weight vector. Thus, we can rewrite the correlation matrix and the correlation vector omitting K as in [14],

$$\hat{R}\mathrm{xx(k)} = \sum_{i=1}^{k}\bar{x}(i)\,\bar{x}^H(\mathrm{i}) \tag{3.14}$$

$$\hat{r}(\mathrm{k}) = \sum_{i=1}^{k}\bar{d}^{*}(i)\,\bar{x}(i) \tag{3.15}$$

Where k is the block length and last time sample k and $\hat{R}$xx(k), $\hat{r}$(k) is the correlation estimates ending at time sample k. Both of the above summations use rectangular windows, thus they equally consider all previous time samples. Since the signal sources can change or slowly move with time, we might want to deemphasize the earliest data samples and emphasize the most recent ones. This can be accomplished by modifying Eqs. (3.14) and (3.15), such that we forget the earliest time samples. This is called a weighted estimate.

Thus

$$\hat{R}\text{xx(k)} = \sum_{i=1}^{k} \alpha^{k-i} \bar{x}(i)\, \bar{x}^{H}(\text{i}) \tag{3.16}$$

$$\hat{r}\text{(k)} = \sum_{i=1}^{k} \alpha^{k-i}\ \bar{d}^{*}(i)\, \bar{x}(i) \tag{3.17}$$

Where α is the *forgetting factor*.

The forgetting factor is also sometimes referred to as the exponential weighting factor [22]. And it is a positive constant. Let us break up the summation in Eqs. (3.16) and (3.17) into two terms: The summation for values up to i = k−1 and last term for i = k.

$$\hat{R}\text{xx(k)} = \alpha \sum_{i=1}^{k} \alpha^{k-1-i} \bar{x}(i)\, \bar{x}^{H}(\text{i}) + \bar{x}(k)\, \bar{x}^{H}(\text{k}) = \alpha\, \hat{R}\text{xx(k-1)} + \bar{x}(k)\, \bar{x}^{H}(\text{k}) \tag{3.18}$$

$$\hat{r}\text{(k)} = \alpha \sum_{i=1}^{k} \alpha^{k-1-i}\ \bar{d}^{*}(i)\, \bar{x}(i) + \bar{d}^{*}(k)\, \bar{x}(k) = \alpha\, \hat{r}\text{(k-1)} + \bar{d}^{*}(k)\, \bar{x}(k) \tag{3.19}$$

Thus, future values for the array correlation estimate and the vector correlation estimate can be found using previous values. The advantage of the recursion approach is that one need not calculate the correlation for an entire block of length K. Rather, each update only requires one a block of length 1 and the previous correlation matrix. After some mathematical formulations as in [14] the weight vector for RLS can be estimated using the following formula.

$$\bar{w}(k) = \bar{w}(k-1) + \bar{g}(\text{k})\left[\bar{d}^{*}(k) - \bar{x}^{H}(\text{k})\bar{w}(k-1)\right] \tag{3.20}$$

Where

$$\bar{g}(\text{k}) = \hat{R}_{xx}{}^{-1}(k)\, \bar{x}(k)$$

Chapter 4: Simulations and Results

4.1 Introduction

In this chapter, performance characteristics of the three non-blind adaptive beamforming algorithms (LMS, RLS & SMI) on the basis of SLL is investigated. For simulation (implementation) of these algorithms MATLAB software is used for programming purpose and the smart antenna radiation pattern (array factor plot) for performance parameters of different inter-element spacing and number of elements of the array will be simulated for the specified algorithms.

Finally, comparison of the three algorithms based on SLL of the array factor plot for the optimum inter-element spacing ($d = 0.5\lambda$) and different number of elements of an array will be presented.

4.2 Simulation parameters

For simulation, a uniform linear array (uniformly spaced array elements) with no coupling between them and narrow band signals induced at array sensors are considered. The Additive White Gaussian Noise channel (AWGN) is considered because of having the same power spectral density for all frequencies and is common to every communication channels. For LMS algorithm, convergence factor of 0.02 is selected because of a too large step size gives a fast response to but results in a large excess mean square error (MSE), and may even cause loss of convergence. A too small step size degrades tracking capabilities of the algorithm. A forgetting factor of relatively close to unity (0.9) for RLS algorithm is also taken in order to achieve low misadjustment and good stability as compared to smaller value. The assumed simulation parameters are summarized in the below table.

Table 4.1: Simulation parameters assumptions

Channel type	Flat fading channel
SNR	10dB
K(No of iterations)	100
μ(Convergence factor)	0.02
α(Forgetting factor)	0.9
Noise	AWGN
Software	MATLAB

4.3 Simulation of array factor pattern for LMS algorithm

For simulation purpose of the LMS algorithm, assuming that the desired signal vector is defined by $x_s(k) = a_0 s(k)$ where s(k) = cos(2$\pi t/T$) with T = 1ms and the interfering signal vector is defined by $x_i(k) = a_1 i(k)$ where i(k) = randn(1,100). Both signals are nearly orthogonal over the time interval T. Let the desired signal d(k) = s(k).

Case I: Array factor (AF) plots of LMS algorithm using spacing between elements d=0.5λ and Ne = 5, 8, 12

The following figure shows normalized array factor plot of a ULA of 5, 8 and 12 elements for a uniform inter-element spacing of 0 .5λ.

It is considered that the desired user signal is arriving at an angle 0° and an interferer at an angle -60°. The array factor for number of elements equal to 5, 8 and 12 is computed and the figure shows the array factor plots and how the LMS algorithm places deep nulls in the direction of interfering signals and maximum in the direction of the desired signal.

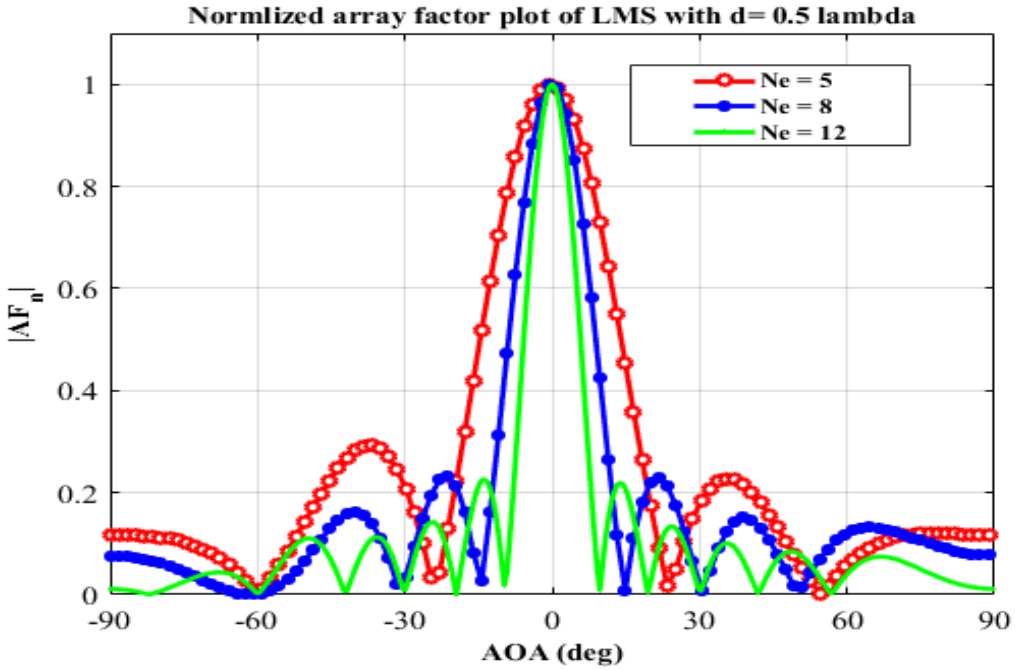

Figure 4.1: Normalized AF plots for LMS algorithm at $\boldsymbol{\theta_d} = 0°$ and $\boldsymbol{\theta_i} = -60°$ with $d = 0.5\lambda$

Therefore, from Figure 4.1, the normalized array factor plots of the longer array (Ne = 12) results a narrow beam width with a sidelobe level of -6.51dB as compared to the other two array (-6.34 dB for Ne = 8 and -5.35 dB for Ne=5).

All the figures are plotted first taking the respective magnitude of the desire and the interferer signal at the respective location from the beam pattern then normalized these values by the maximum one. After that, the values of the SLL (in dB) at any angle is calculated by first taking its linear value from the normalized AF pattern and then converting this value using conversion formula,

$$\text{AF(dB)} = 10 * \log(linear\ value) \tag{4.1}$$

The corresponding complex weights for each of the arrays plotted in Figure 4.1 are calculated using Eq. (3.5) and then normalizing the result to the first weight gives the values shown in Table 4.2. These values are calculated during simulation of the AF pattern using the MATLAB software. The values are the normalized optimum weights which are found when the LMS algorithm converges after 60 iterations.

Table 4.2: Array weights for LMS algorithm with $d = \lambda/2$ at $\theta_d = 0°$ and $\theta_i = -60°$

No. of elements (Ne)	Weights
5	w_1 = 1, w_2 = 1.1634-0.13775i, w_3 = 0.95798-0.078795i w_4 = 1.1696 - 0.048662i, w_5 = 0.98876 - 0.16262i
8	w_1 = 1, w_2 = 1.2695+0.089999i, w_3 = 1.0603-0.10226i, w_4 = 1.1727+0.1587i, w_5 = 1.1767-0.12541i, w_6 = 1.057+0.13225i, w_7 = 1.2715-0.053988i, w_8 = 0.9996+0.028329i
12	w_1 = 1, w_2 = 1.0842-0.053764i, w_3 = 0.98538-0.039083i w_4 = 1.0815-0.012119i, w_5 = 1.0048-0.076022i w_6 = 1.0487+0.013666i, w_7 = 1.0453-0.086151i w_8 = 1.0077+0.006372i, w_9 = 1.0798-0.062707i w_{10} = 0.98573-0.02913i, w_{11} = 1.0853-0.021344i w_{12} = 0.9976-0.069134i

Figure 4.2 shows the plot of weight versus iteration number for an array of Ne = 5 to the above normalized array factor plot of the same parameters. The plot shows how the values of weights varying until the algorithm converges. From the figure, it is observed that the LMS algorithm converges after 60 iterations. This shows the LMS algorithm converges slowly even if it is the simplest one in terms of complexity as compared to the other two algorithms that would be discussed in next section.

The convergence of the algorithm after 60 iterations is clearly indicated as the magnitude of the weights become constant when the number of iteration extends beyond this value of iteration.

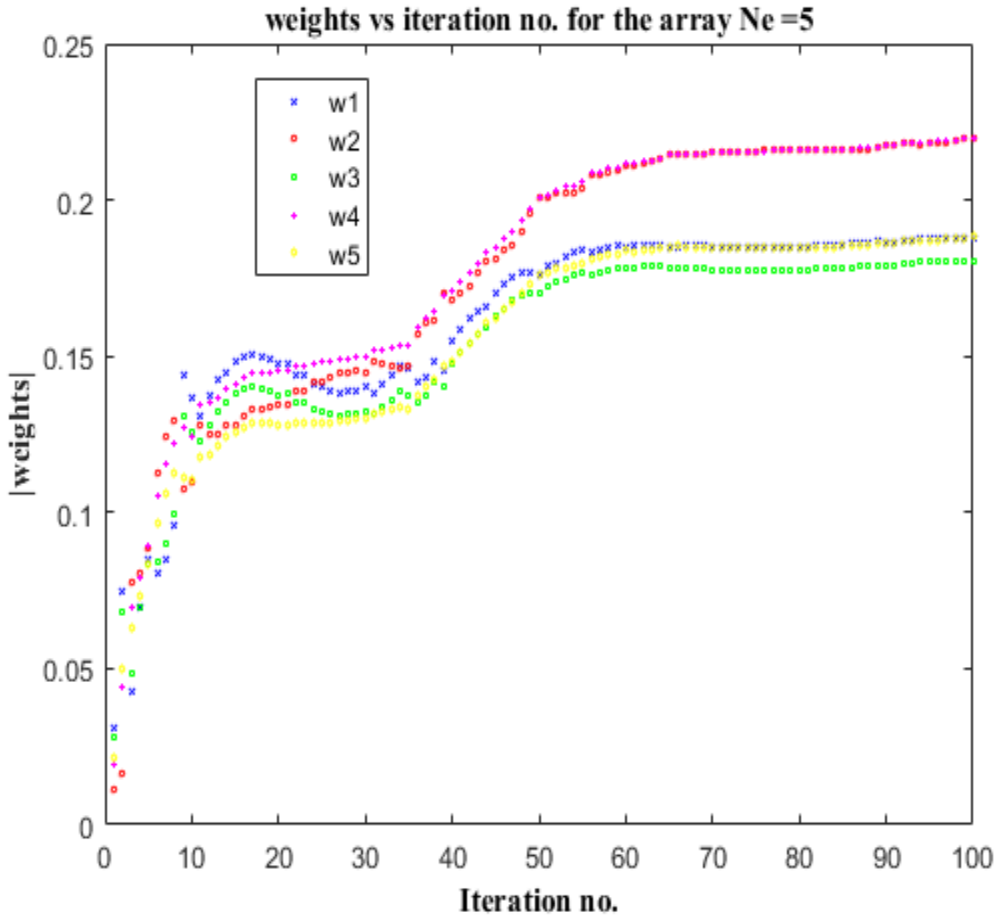

Figure 4.2: Weight vs Iteration number plot of LMS algorithm for Ne =5 and $d = 0.5\lambda$

Figure 4.3 shows the plot of desired and array output signals versus number of iterations for each of the three array antennas. From this figure also, one can deduce that, the LMS algorithm does not converge until 60 iterations as it was investigated from the weight versus iteration number plot.

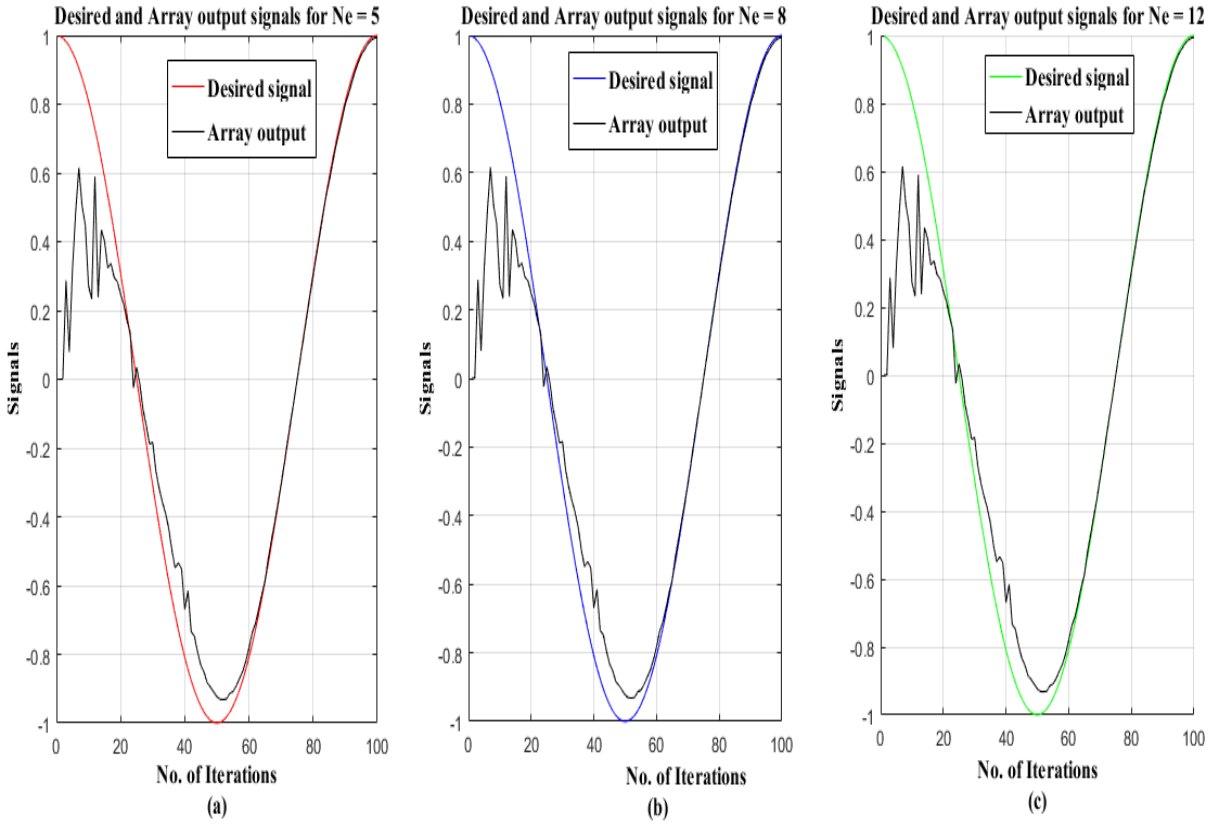

Figure 4.3: Plot of desired and array output signal versus No. of iterations (a) Ne=5, (b) Ne = 8, and (c) Ne = 12

For the same parameters of the above arrays, the graphical characteristics of the mean square error versus number of iteration is reflected on the following figure.

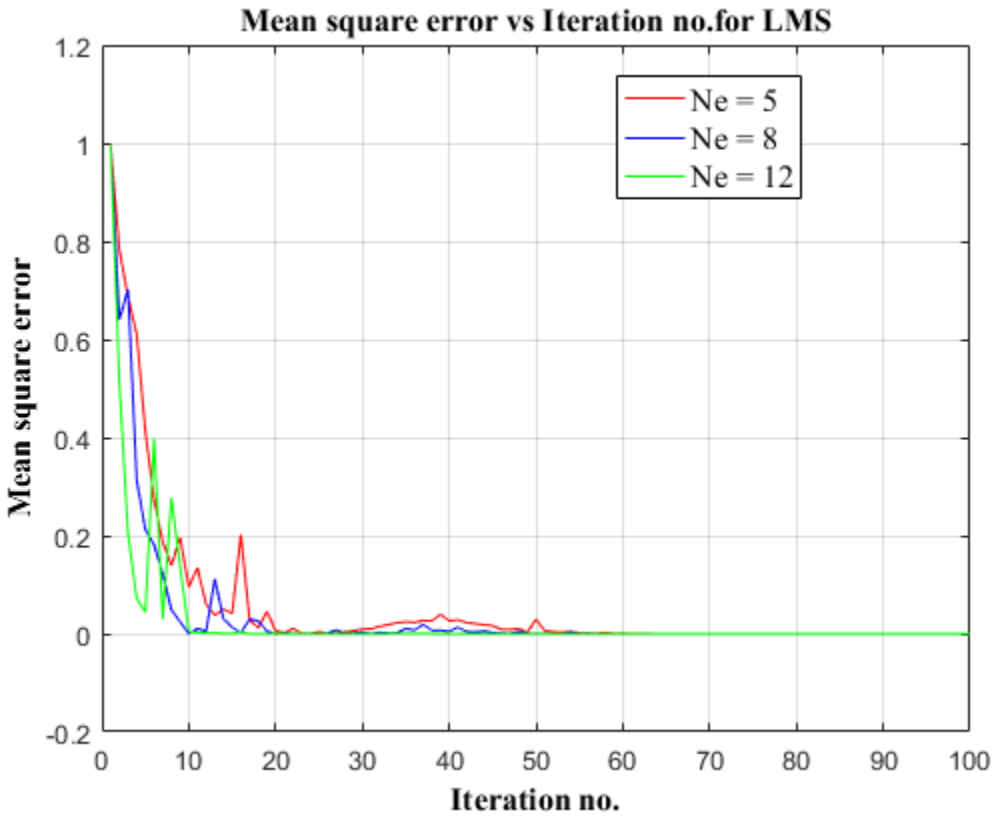

Figure 4.4: MSE versus number of iteration for LMS algorithm for fixed $d=\boldsymbol{\lambda/2}$ and Ne = 5, 8 and 12.

The array factor plot for different direction of arrival of the desired and interferer signal for the same parameters as before ($d = 0.5\lambda, Ne = 5, 8, 12$) is shown in next figures.

From the two array factor plots shown in figure 4.5, for fixed inter-element spacing between elements ($d = 0.5\lambda$), we can reach at the same conclusion as before. That means, as the number of elements increases, a narrow beam is directed towards the desired user direction and the interferer is suppressed by placing deep nulls at its direction of arrival.

Comparing Figure 4.1 and 4.5, for Ne = 8 and 12, there is almost identical maximum SLL characteristics of all the three figures. When the number of elements become five there is creation of two maximum sidelobes as in Figure 4.5 (a) with different angle of arrival of both desired and interferer signals from Figure 4.1.

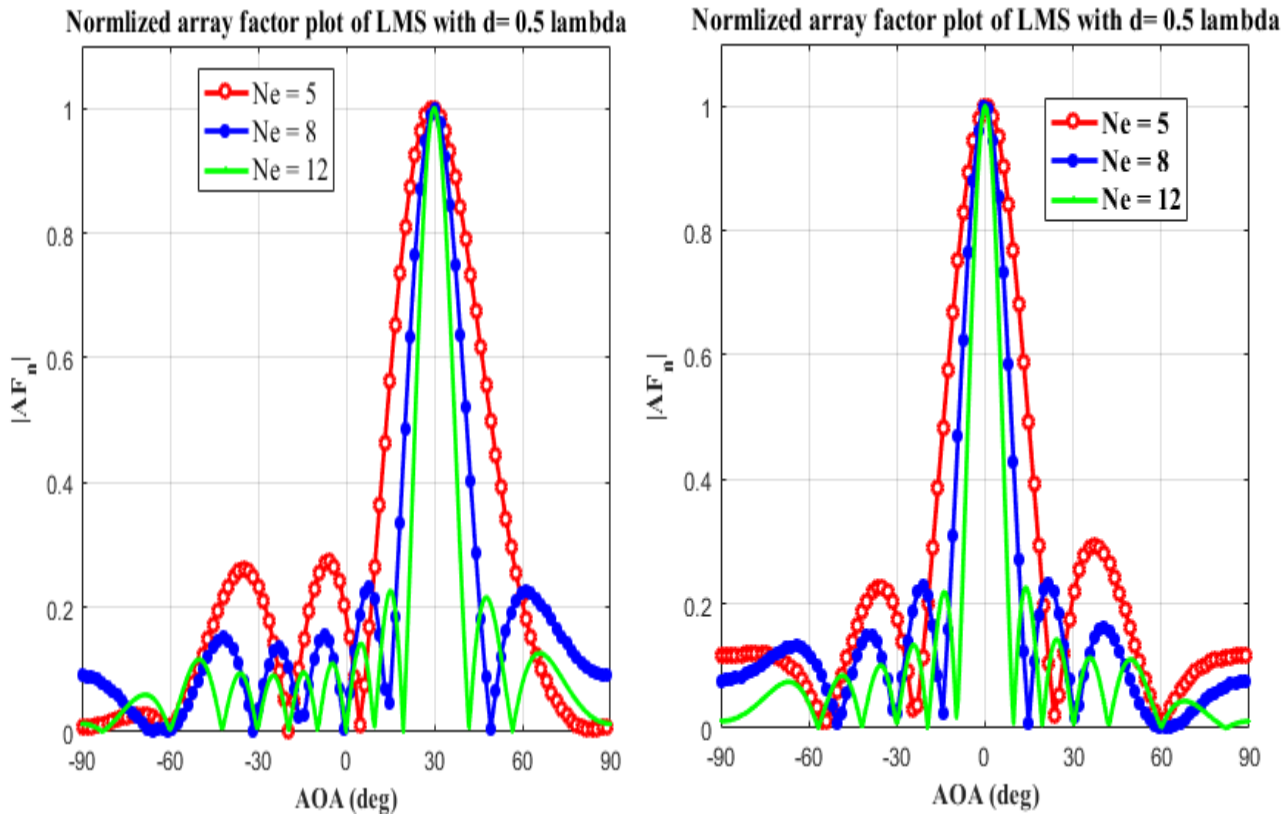

(a) (b)

Figure 4.5: Normalized AF plot for LMS algorithm with $d=0.5\lambda$ at (a) $\boldsymbol{\theta_d} = 30°$ and $\boldsymbol{\theta_i} = -60°$ and (b) $\boldsymbol{\theta_d} = 0°$ and $\boldsymbol{\theta_i} = 60°$

Case II: Array factor (AF) plots of LMS algorithm with spacing between elements $d=0.25\lambda$ and Ne = 5, 8, 12

From the plot shown in Figure 4.6, as the separation between the elements becomes half of the first case, there is challenge of having a broad beam in the direction of desired user. Having this type of antenna pattern (broad main beam) leads to more interference for mobile communication. For this case of spacing, there is no a much benefit of reducing the sidelobe level of the arrays.

For different angle of arrival of the desired user signal and interferers the same conclusion can be drawn as illustrated in the next few plots of the array factor for the same parameters of the smart antenna that can be used for wireless communication system.

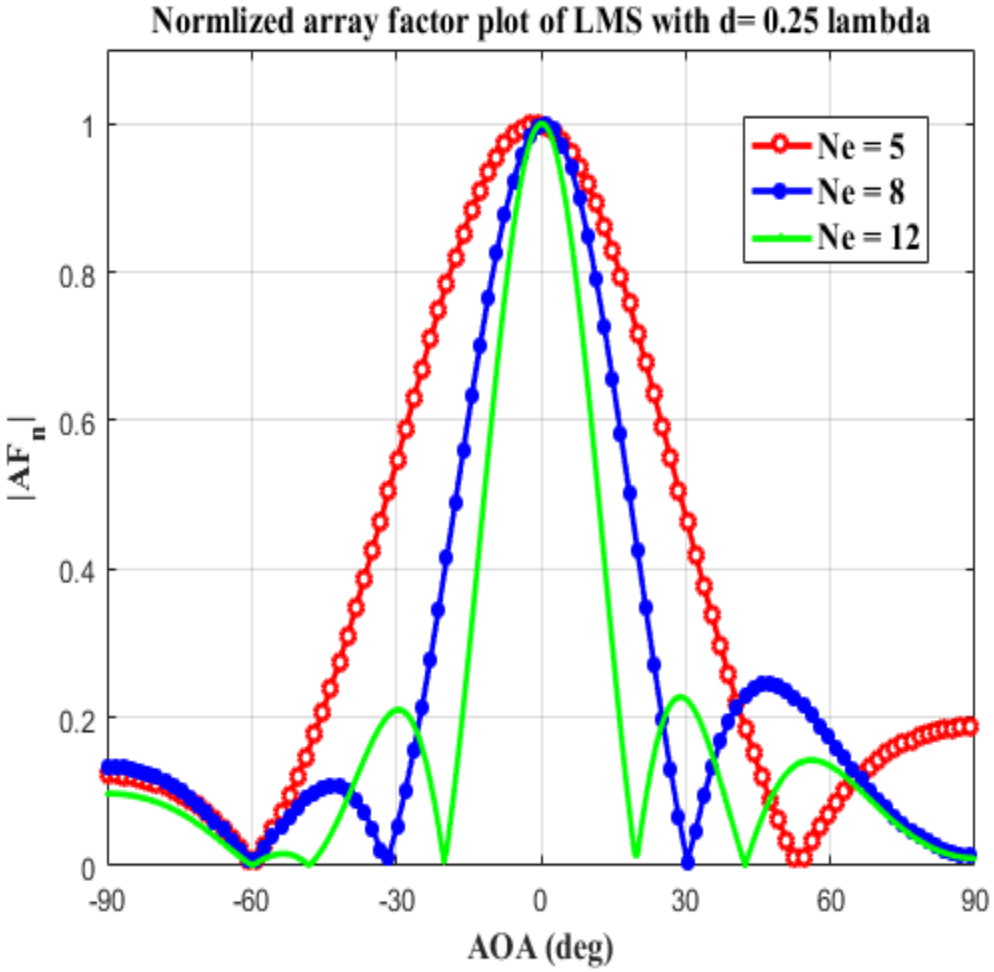

Figure 4.6: Normalized AF plot of LMS for $d=0.25\lambda$, Ne =5, 8 and 12 $at\ \boldsymbol{\theta_d}$ = 0° & θ_i= -60°

For different angle of arrival of desired signal (30°) and interferer (-60°), Figure 4.7 shows the normalized array factor plot having the same properties as the above plot.

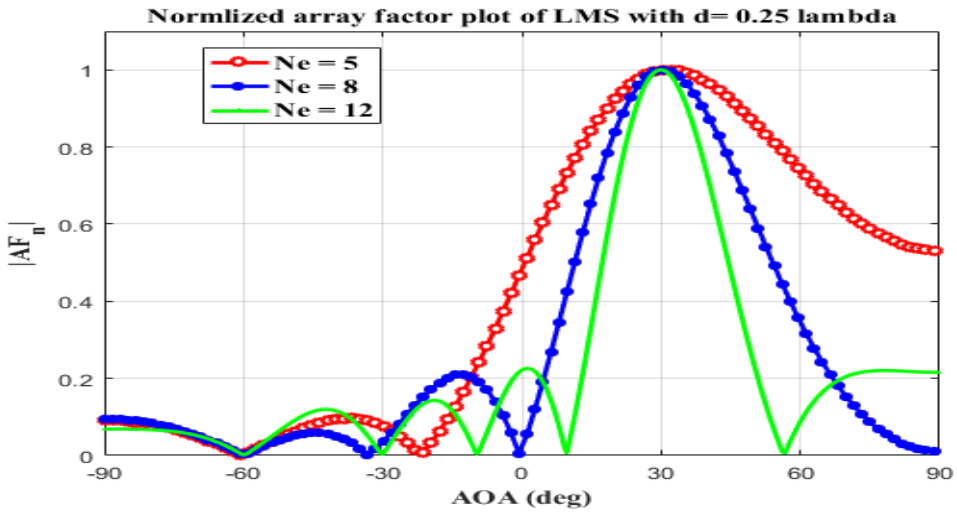

Figure 4.7: Normalized AF plot of LMS for $d=0.25\lambda$, Ne =5, 8 and 12 at $\boldsymbol{\theta_d}$ =30° & $\boldsymbol{\theta_i}$=-60°

Case III: Array factor (AF) plots of LMS algorithm with spacing between elements $d=0.75\lambda$ and Ne = 5, 8, 12

When the spacing between the elements increases beyond 0.5λ and becomes 0.75λ, the array factor plot is illustrated in the following plot.

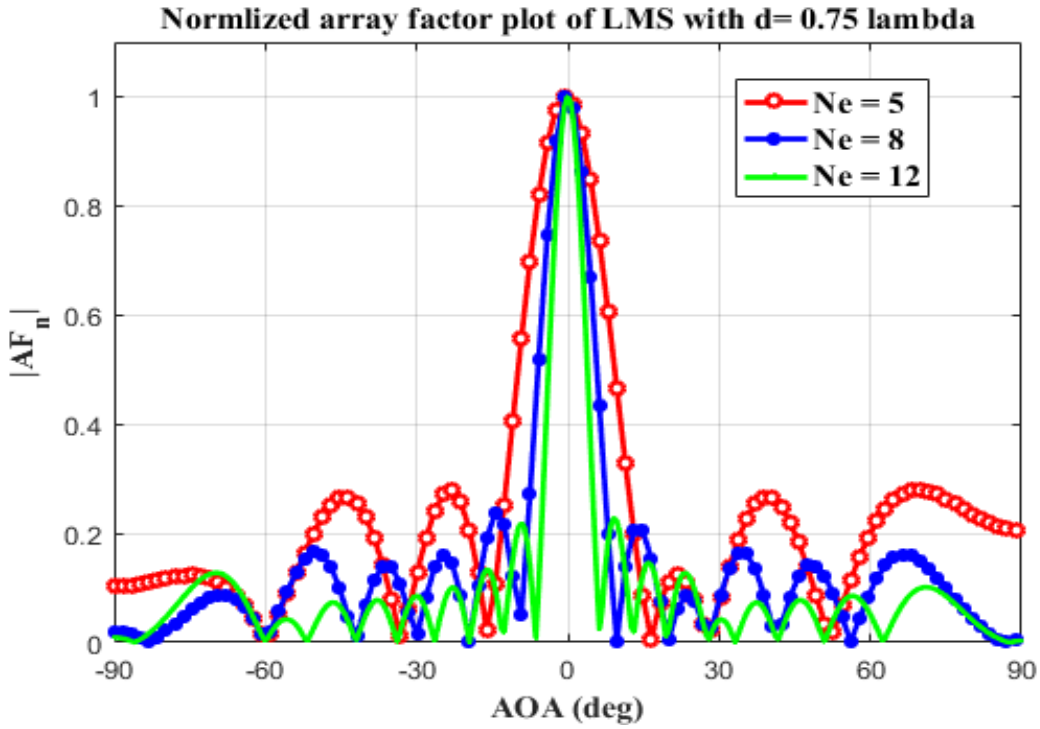

Figure 4.8: Normalized AF plot of LMS algorism for $d=0.75\lambda$ with $\boldsymbol{\theta_d}$ = 0° and $\boldsymbol{\theta_i}$= -60°

As seen from Figure 4.8, even if there is a narrow beam as the number of elements increase, there are large number of sidelobes and grating lobes may occur due to large spacing between the elemens. This leads to poor performance of the smart antenna system.

For all of the three cases *((d = 0.75, 0.5, 0.25) λ)* the sidelobe level characteristics can be summarized as follows.

Table 4.3: Array factor SLL comparison for LMS algorithm for *d = (0.75, 0.5, and 0.25) λ*

DOA of desired signal (θ_d)	DOA of interferer signal (θ_i)	Inter-element spacing *(d)*	Number of element in the array (Ne)	AF pattern SLL (in dB)
0°	-60°	$d = 0.75\lambda$	5	-5.54
			8	-6.27
			12	-6.43
		$d = 0.5\lambda$	5	-5.35
			8	-6.34
			12	-6.51
		$d = 0.25\lambda$	5	-7.3
			8	-6.12
			12	-6.44

From the Table 4.3, the SLL shows an oscillating manner by some level as the distance between elements decreases for the corresponding number of elements. Reducing the spacing also creates a problem of having a broad main beam which is not required for reliable communication.

Considering the first two largest inter-element spacing, for number of elements Ne = 8 and 12, the spacing distance $d = 0.5\lambda$ and Ne =12 provides an optimum solution in terms of SLL as compared to the spacing $d = 0.75\lambda$. The smallest spacing $d = 0.25\lambda$ and number of elements Ne = 5 creates a very wide beam which is not recommended for decreasing the interference of a wireless communication system. These performance characteristics are investigated in previous plots of the LMS algorithm.

Case IV: AF plots of LMS algorithm with fixed Ne and varying distance *(d)*

The AF plot for the number of elements equal to five, eight and twelve with inter-element spacing of 3λ/4, λ/2 and λ/4 is computed. The following three figures show these plots.

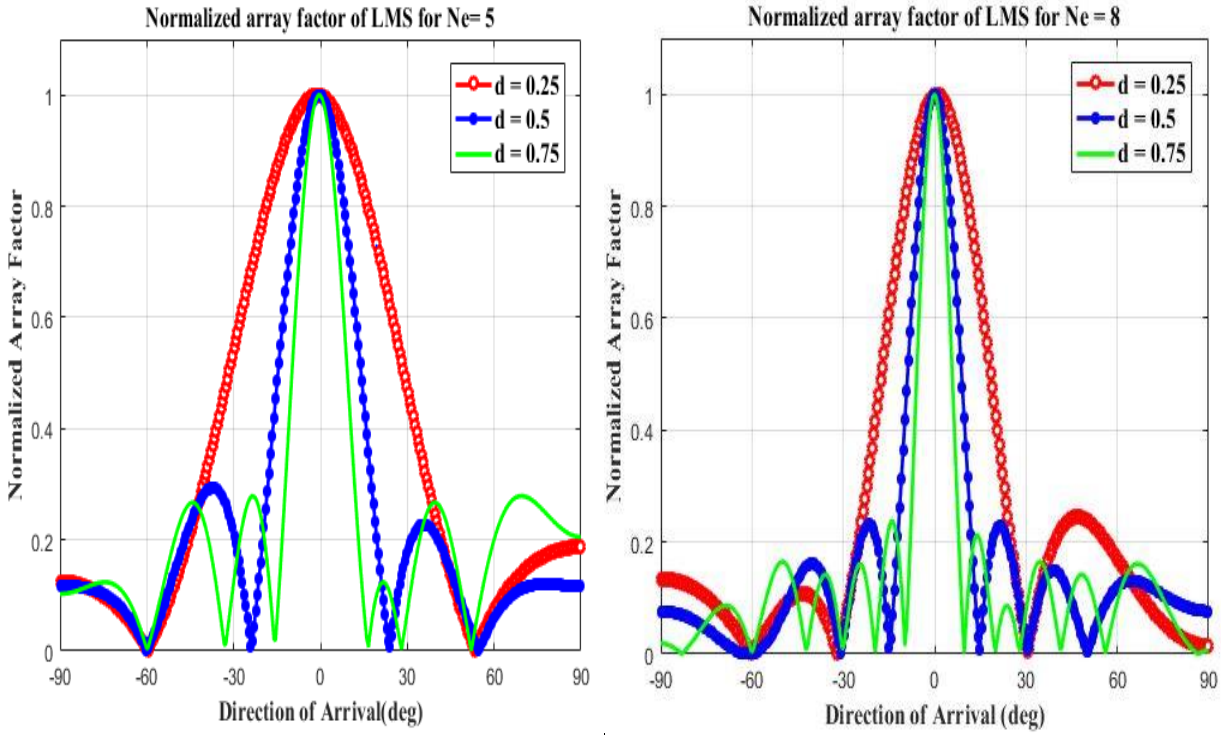

(a) (b)

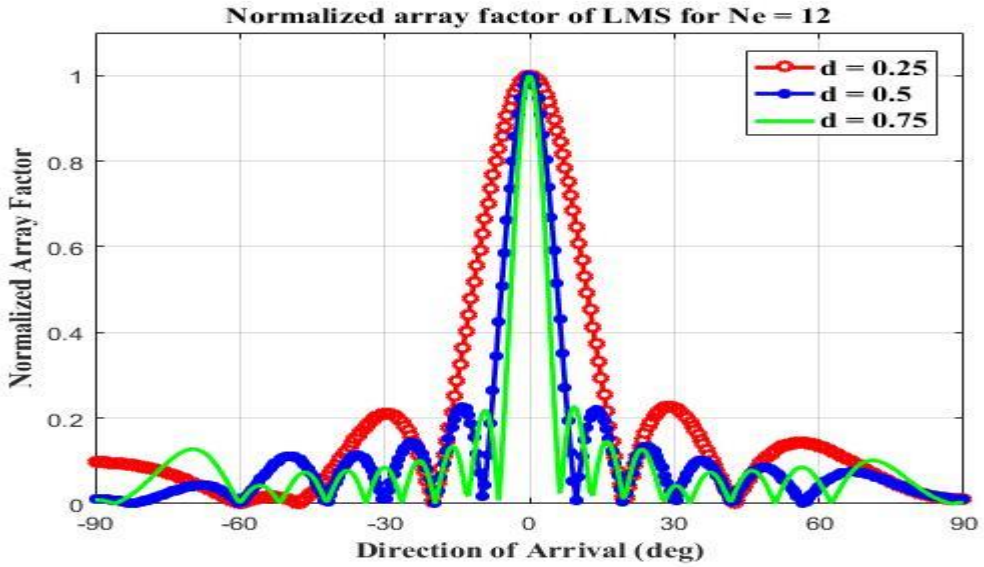

(c)

Figure 4.9: AF plots of LMS algorithm with fixed number of element and varying *d*

From Figure 4.9, it is cear that the spacing $d = 0.5\lambda$ gives an optimum result interms of directivity and maximum value of sidelobe. As the number of elements in the array increases, a narrow beam

is directed towards the desired user which is the goal of any smart antenna in reducing interference.

From Figure 4.9 (c), which is the AF plot of LMS algorithm for three different inter-element spacing and fixed N_e = 12, one can observe that the number of sidelobes are increasing with increasing the spacing between the elements.

As compared to *d = 0.75λ,* for the inter-element spacing *d = 0.5λ*, there is no grating lobe and also there are small number of sidelobes with wider beamwidth. For large angle of separation which is the difference in angular separation between the DOA of the desired and the interferer (when this separation is greater than half of the first beam width), the spacing *d=0.5λ* gives a better performance as many papers suggests which is described in [12]. Also in [12], the spacing *d=0.5λ* is optimal only for angle of separation larger than half of the first beam width. Unlike for large angle of separation increasing the spacing between array elements gives a better performance for small angle of separation.

Since the magnitude of angle of separation between the DOA of the desired and the interferer signal in Figure 4.9 (c) is (0° -(-60°) = 60°) which is greater than half of the first null beamwidth having a value about 6°, the spacing *d = 0.5λ* is the optimum one as compared to the other separation distances between array elements. It is also clear from the figure that this spacing is the best alternative interms the width of the beam and number of sidelobes (considering both simultaneously) as compared to the other two separation distances.

4.4 Simulation of array factor pattern for SMI algorithm

For simulation purpose of the SMI algorithm, assuming that the same signals parameters like that of the LMS algorithm, the desired signal vector is defined by the same as that of LMS $x_s(k) = a_0 s(k)$ where s(k) = cos(2$\pi t/T$) with T = 1mS. Let the block length be K=100 such that t = (0:100)*T/k and the interfering signal vector is defined by $x_i(k) = a_1 i(k)$ where i(k) = randn(1,K). Also assume the desired signal d(k) = s(k) for keeping the correlation matrix inverse from becoming singular, by adding noise to the system with variance ${\sigma_n}^2 = 0.01$. Simulation of the AF for different cases is illustrated in the following plots.

Case I: Array factor (AF) plots of SMI algorithm using $d = 0.5\lambda$ and Ne= 5, 8 and 12

The following plot shows how the number of elements of the array affect the beam pattern of smart antennna that uses the SMI algorithm as its beamforming method for its digital signal processing unit.

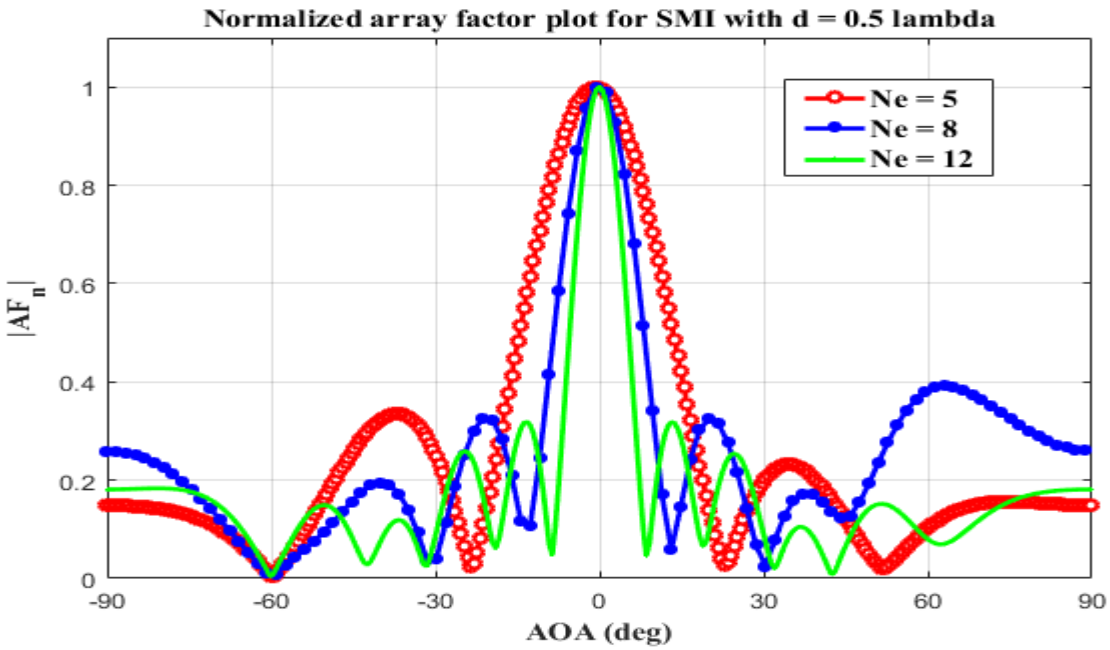

Figure 4.10: Normalized AF plot for SMI algorithm with $d=0.5\lambda$ at $\boldsymbol{\theta_d = 0° \; and \; \theta_i = -60°}$

From the two plots of Figure 4.1 and 4.10, which are the corresponding plots of LMS and SMI algorithms with same parameters respectively, the LMS algorithm produces the lower maximum SLL as compared to the SMI algorithm. This is verified by comparing the maximum SLL of the array factor plot for corresponding number of elements of each algorithm.

For different angle of arrival of the desired and interferer signal from Figure 4.10, the array factor plot for SMI algorithm is plotted as shown in Figure 4.11.

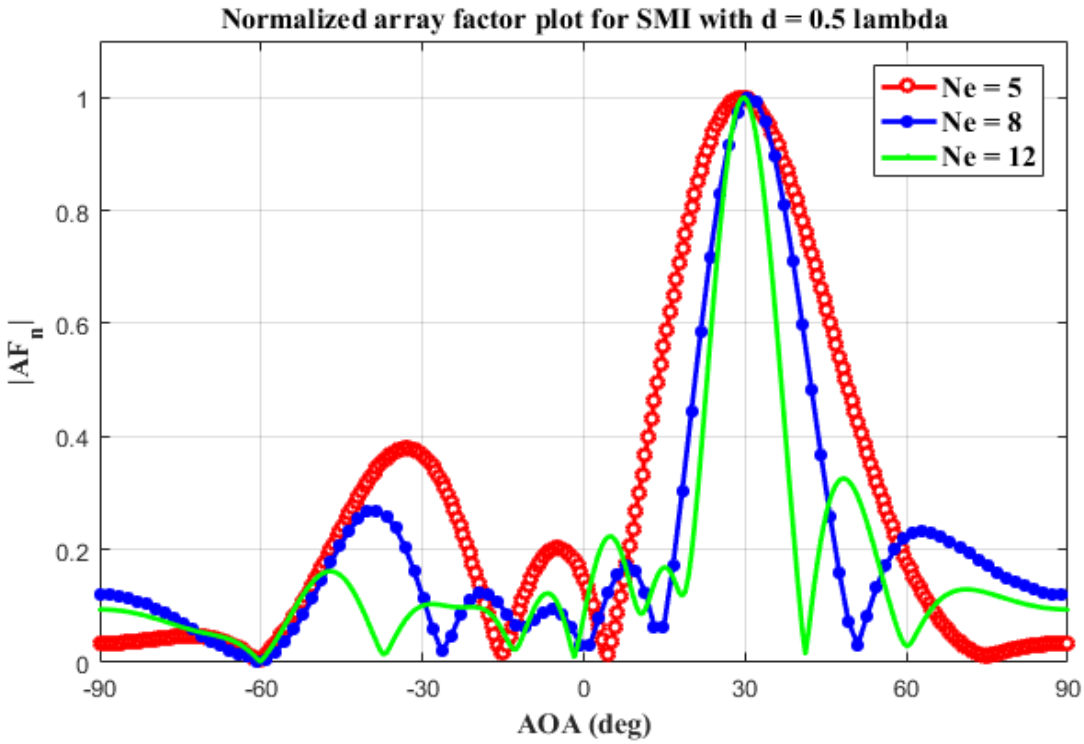

Figure 4.11: Normalized AF plot for SMI algorithm with $d=0.5\lambda$ at $\boldsymbol{\theta_d = 30° \; and \; \theta_i = -60°}$

Comparison of Figure 4.11 with Figure 4.5 (a) results that the AF plot shown in Figure 4.5 (a) has better performance in terms producing lower SLL. This also reflects the good performance characteristics of the LMS algorithm in terms of sidelobe level for same parameters of algorithms.

The above two plots of SMI algorithm show how the number of elements of the array affects the radiation pattern of smart antenna system. Similar to that of the LMS algorithm, for SMI algorithm, a narrow beam is obtained by increasing the number of elements for a fixed inter-element spacing.

Case II: AF plot of SMI algorithm using $d = 0.25\lambda$ and Ne= 5, 8 and 12

The two plots of SMI algorithm shown in Figure 4.12 indicates that, as the spacing between elements decreases by half of the first case a broad beam is created which leads to poor communication for smart antenna system.

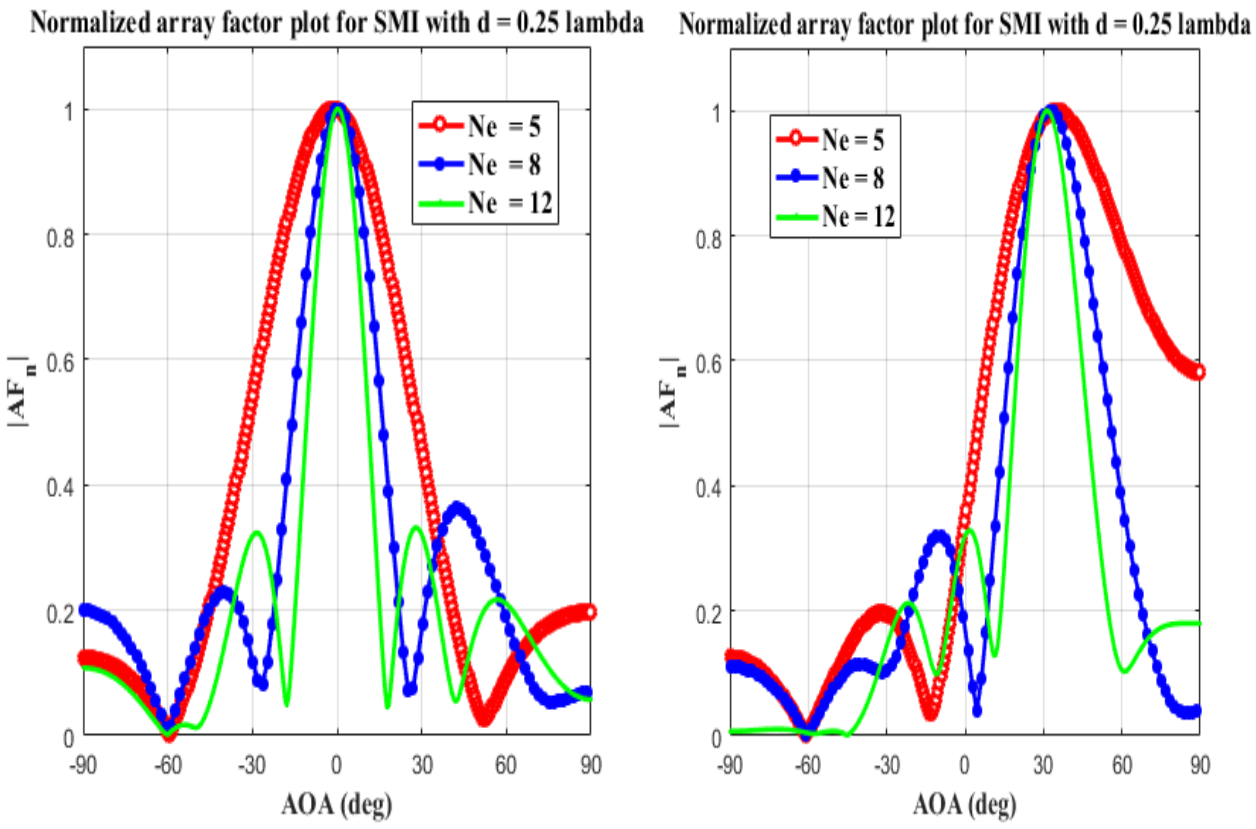

(a) (b)

Figure 4.12: AF Plot of SMI with *d=0.25λ*, (a) at $\boldsymbol{\theta_d = 0° \; and \; \theta_i = -60°}$ (b) at $\boldsymbol{\theta_d = 30° \; and \; \theta_i = -60°}$

Comparative analysis of Figure 4.12 and Figure 4.6 reveals that, for same array parameters, the two arrays Ne = 8 and 12 produce larger maximum sidelobe in the case of Figure 4.12. This shows that the superiority of LMS algorithm (with performance criterion of SLL) over the SMI algorithm when the inter-element spacing becomes 0.25λ.

Case III: AF plot of SMI algorithm using $d = 0.75\lambda$ and Ne= 5, 8 and 12

When the spacing between the elements exceeds above the half wavelength and becomes equal three fourth of the wavelength a narrow main beam with large number of sidelobes is created as shown in plots of Figure 4.13. Also Figure 4.13 (b) illustrates when the spacing increases beyond the half wavelength there is creation of grating lobes which degrades performance of communication system.

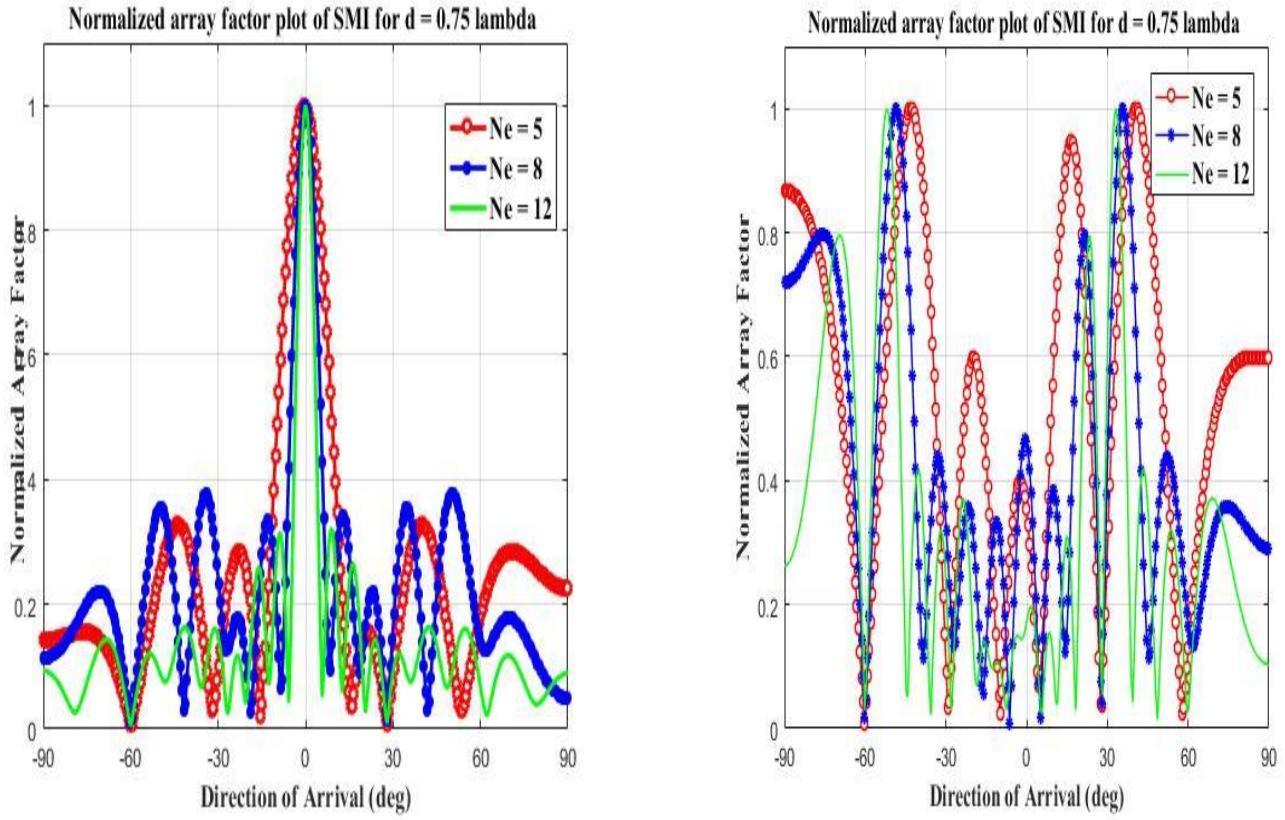

(a) (b)

Figure 4.13: Normalized AF plot for SMI algorithm with *d=3λ/4*, (a) at $\theta_d = 0°$ *and* $\theta_i = -60°$ (b) at $\theta_d = 30°$ *and* $\theta_i = -60°$

Like LMS, the SLL for the smart antenna that uses SMI algorithm with different inter-element spacing for Ne =12 can be summarized in the following table.

Table 4.4: AF sidelobe level comparison for SMI algorithm at *d = (0.75, 0.5, and 0.25) λ,* Ne = 12

DOA of desired signal (θ_d)	DOA of interferer signal (θ_i)	Element spacing *(d)*	Number of elements (Ne)	AF pattern SLL (in dB)
0°	-60°	*d = 0.75λ*	*12*	*-4.96*
		d = 0.5λ	*12*	*-4.89*
		d = 0.25λ	12	-4.80

As seen from the table, the magnitude of sidelobe seems increasing as the inter-element spacing decreases resembling almost the same magnitude as that of the RLS algorithm will be discussed next.

Comparing Table 4.3 and 4.4 for an array of having twelve elements, for the same spacing and DOA of this array, the LMS algorithm shows lower SLL as compared to SMI algorithm. The characteristics of having lower SLL of LMS algorithm can be taken as its good performance for reducing radiation in unintended direction.

Case IV: AF plot of SMI algorithm for Ne = 12 and d = 0.75λ, 0.5λ and 0.25λ

The figure below depicts the effect of inter-element spacing on the array factor of smart antenna system with an array of twelve elements. This array is selected because of its optimal characteristics in terms of producing a narrow beam as compared to the other two array antennas. The same conclusion can be drawn for the other two arrays (Ne = 5 and Ne = 8) in their normalized array factor pattern with different spacing between the elements. It is also clear that like the other two algorithms the spacing $d = 0.5\lambda$ produces an optimum beam towards the desired direction and it suppresses the interferer by placing nulls at its direction of arrival. If the spacing is increased to more than half wavelength, large sidelobes begin to appear in the radiation pattern. However, the central beam gets narrower because the overall length of the antenna has increased. The radiation pattern is shown in Figure 4.14.

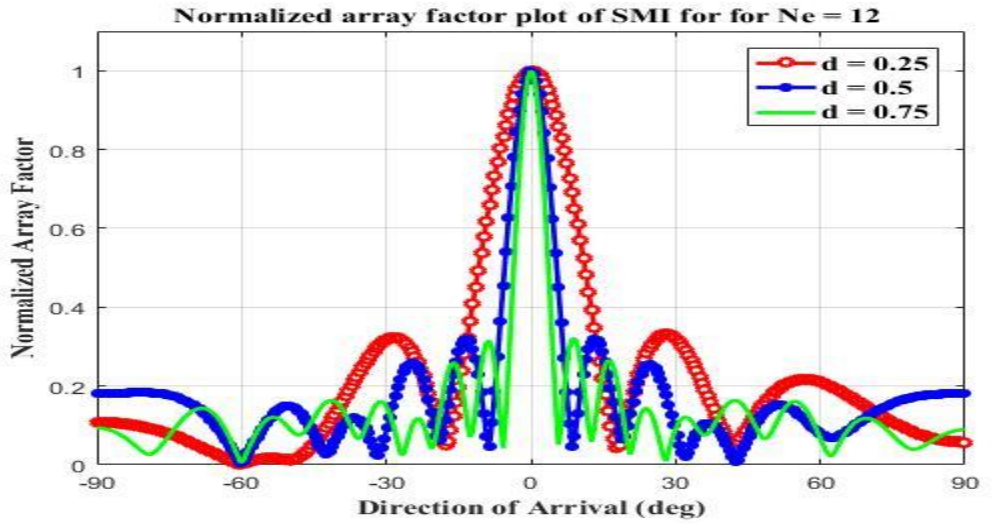

Figure 4.14: AF plots for SMI algorithm for (Ne =12) and varying d at $\theta_d = 0°$ and $\theta_i = -60°$

The plot in Figure 4.9 (c) shows better performance characteristics in terms of SLL as compared to the plot shown in Figure 4.14.

4.5 Simulation of array factor pattern for RLS algorithm

For simulation purpose of the RLS algorithm, assuming that the desired signal vector is defined by the same as that of the other two algorithms.Taking k = 100 time samples and the forgetting factor of 0.9. For different cases, the array factor plots are illustrated in the following sections.

Case I: Array factor (AF) plots of RLS algorithm using $d = 0.5\lambda$ and Ne= 5, 8 and 12

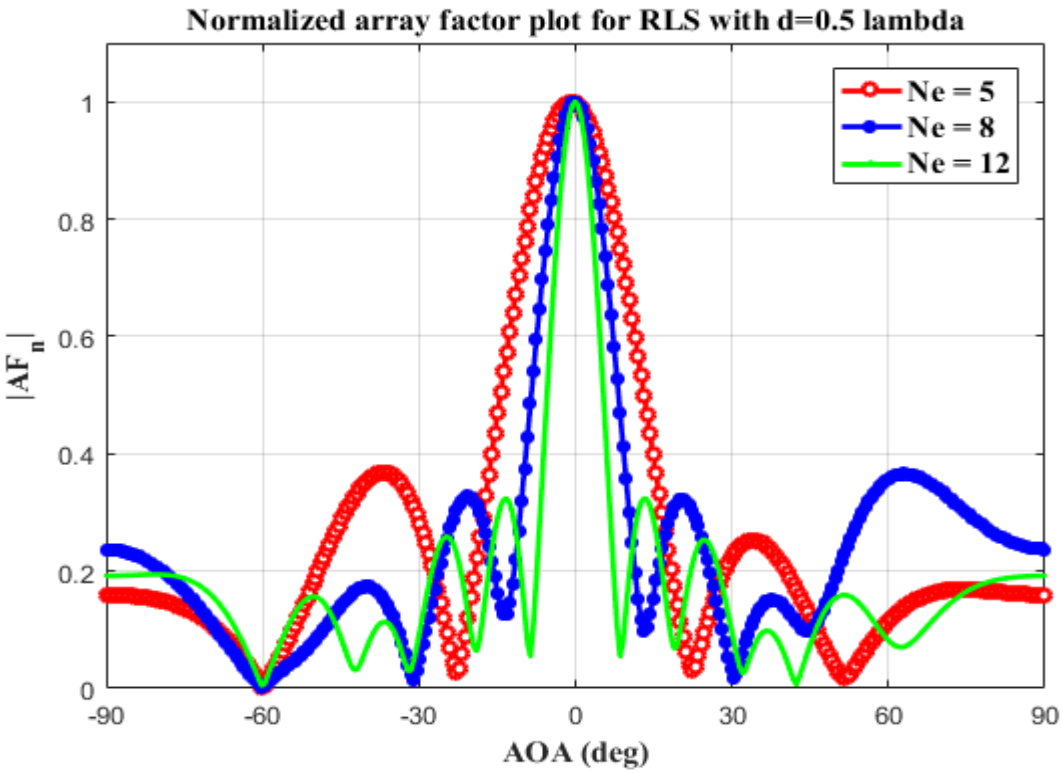

Figure 4.15 :Normalized AF plot for RLS algorithm with $d = 0.5\lambda$, at $\theta_d = 0°$ and $\theta_i = -60°$

From Figure 4.15, the RLS algorithm produce larger maximum sidelobe for Ne = 5 as compared to Figure 4.1 and 4.10. For an array with number of elements equal to eight, Figure 4.15 shows better performance of RLS algorithm than the SMI algorithm which is shown in Figure 4.10. From the corresponding figures of the three algorithms with the same parameter, the LMS shows superiority in terms lower SLL for same types of arrays.

The normalized AF plot at different angle of arrival of the desired and interferer signal is shown in the following plots of RLS algorithm. As shown in Figure 4.16 and 4.17, the main beamwidth is almost the same as that of the first one because of the same array parametrs used for simulation of the AF pattern.

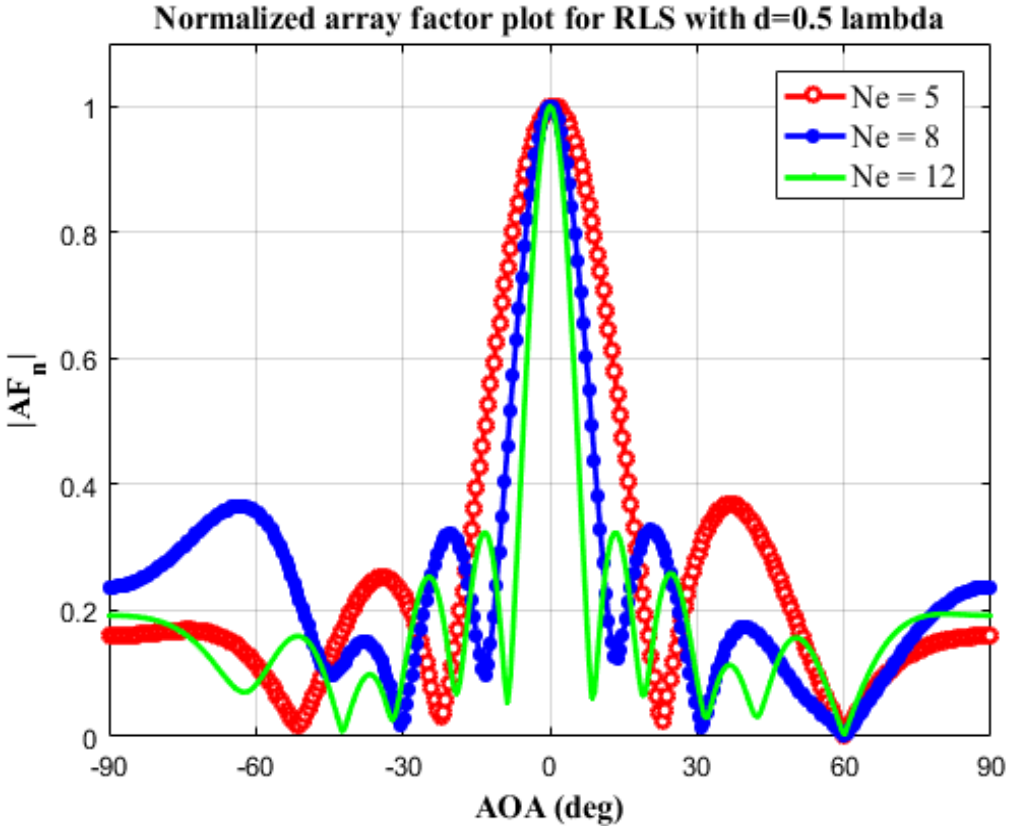

Figure 4.16 :Normalized AF plot for RLS algorithm with *d=0.5λ* at $\boldsymbol{\theta_d = 0° \; and \; \theta_i = 60°}$

The normalized AF plot for $\theta_d = 30° \; and \; \theta_i = -60°$ takes the following form shown in Figure 4.17.

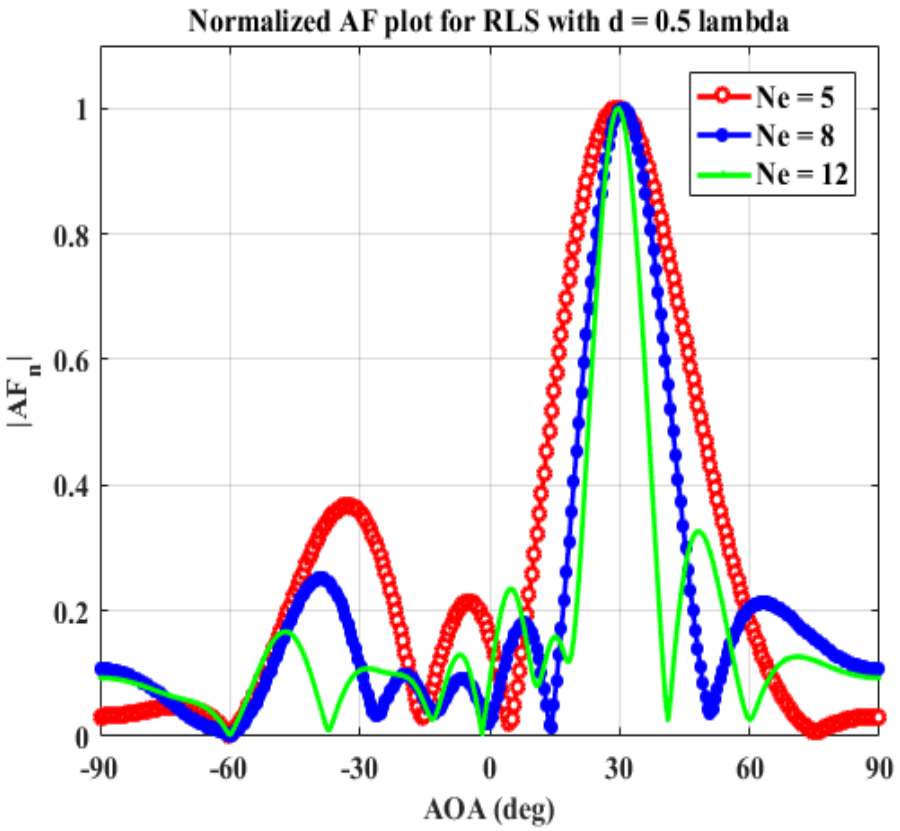

Figure 4.17: Normalized AF plot for RLS algorithm with $d = 0.5\lambda$ at $\boldsymbol{\theta_d = 30° \; and \; \theta_i = -60°}$

From the plot, it is cear that as the number of elemnets increased, anarrow beam is directed towards the desired user at the cost of large number of sidelobes while the interferer is suppressed by placing a deep null at its DOA.

Case II: AF plot of RLS algorithm using $d = 0.25\lambda$ and Ne= 5, 8 and 12

The AF plot when spacing is reduced by half from the first case is shown in the next two plots.

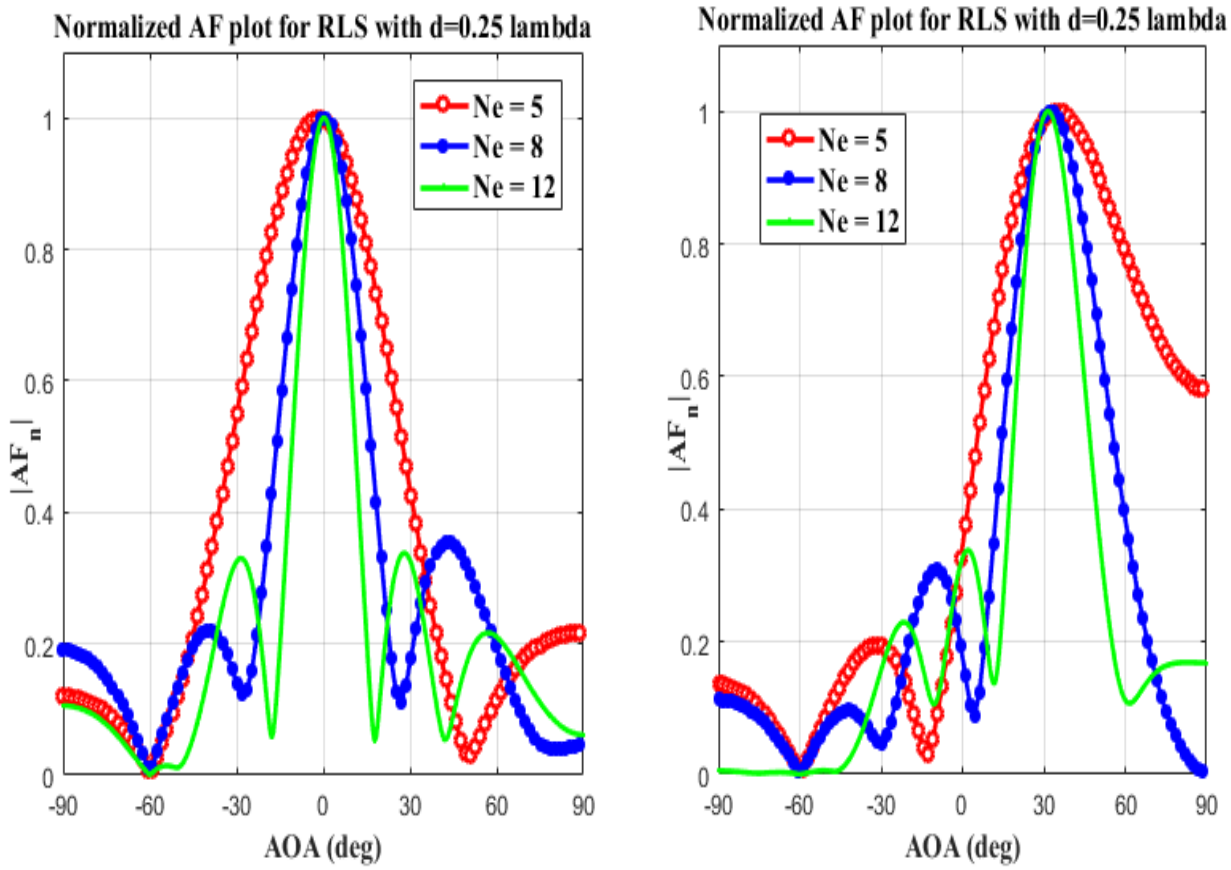

(a) (b)

Figure 4.18: Normalized AF plot for RLS algorithm with $d=0.25\lambda$, (a) at $\theta_d = 0°$ and $\theta_i = -60°$ (b) at $\theta_d = 30°$ and $\theta_i = -60°$

From the above two plots the beamwidth becomes wide as compared to the first case leading more interference.

Case III: AF plot of RLS algorithm using $d = 0.75\lambda$ and Ne= 5, 8 and 12

When there is more spacing beyond the half wavelength (*i.e* $d = 0.75\lambda$) between elements as compared to the previous two cases, the normalized array factor takes the following shape having a relatively narrow beamwidth.

The two plots shown in Figure 4.19 provides the conclusion that, as the spacing between the elements becomes three fourth of the wavelength, a narrow beam is created with a relatively large number of sidelobes. Similar to that of the previous two algorithms, a narrow beam is achived when the number of elements becomes twelve with optimum spacing between elements $d = 0.5\lambda$.

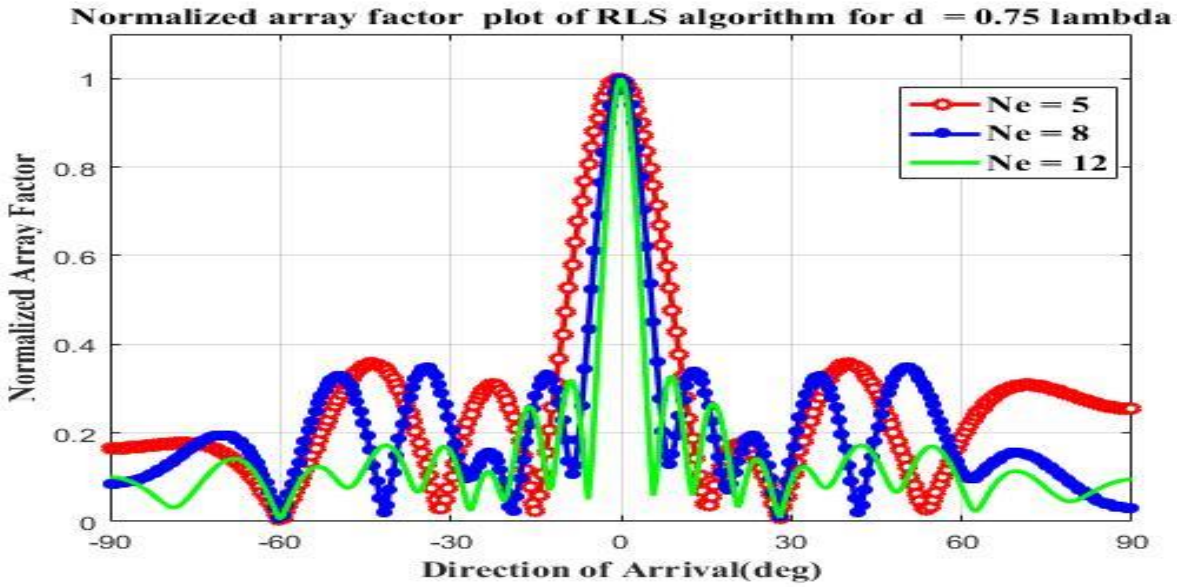

(a)

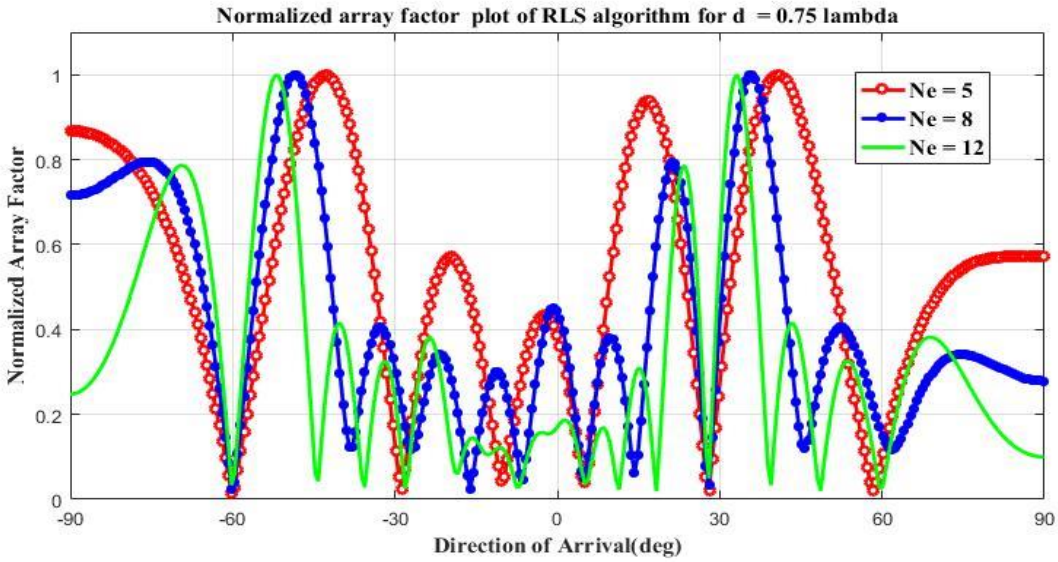

(b)

Figure 4.19: Normalized AF plot of RLS for $d = 0.75\lambda$, at (a) $\theta_d = 0°\ and\ \theta_i = -60°$, (b) $\theta_d = 30°\ and\ \theta_i = -60°$

Case IV: AF plot of RLS algorithm for Ne = 12 and d = 0.75λ, 0.5λ and 0.25λ

The effect of inter-element spacing on the array factor pattern for a fixed number of elements Ne = 12 which is selected for making a narrow beam towards the desired user direction as compared to the other two array types (Ne =5 and Ne = 8) is shown in Figure 4.20.

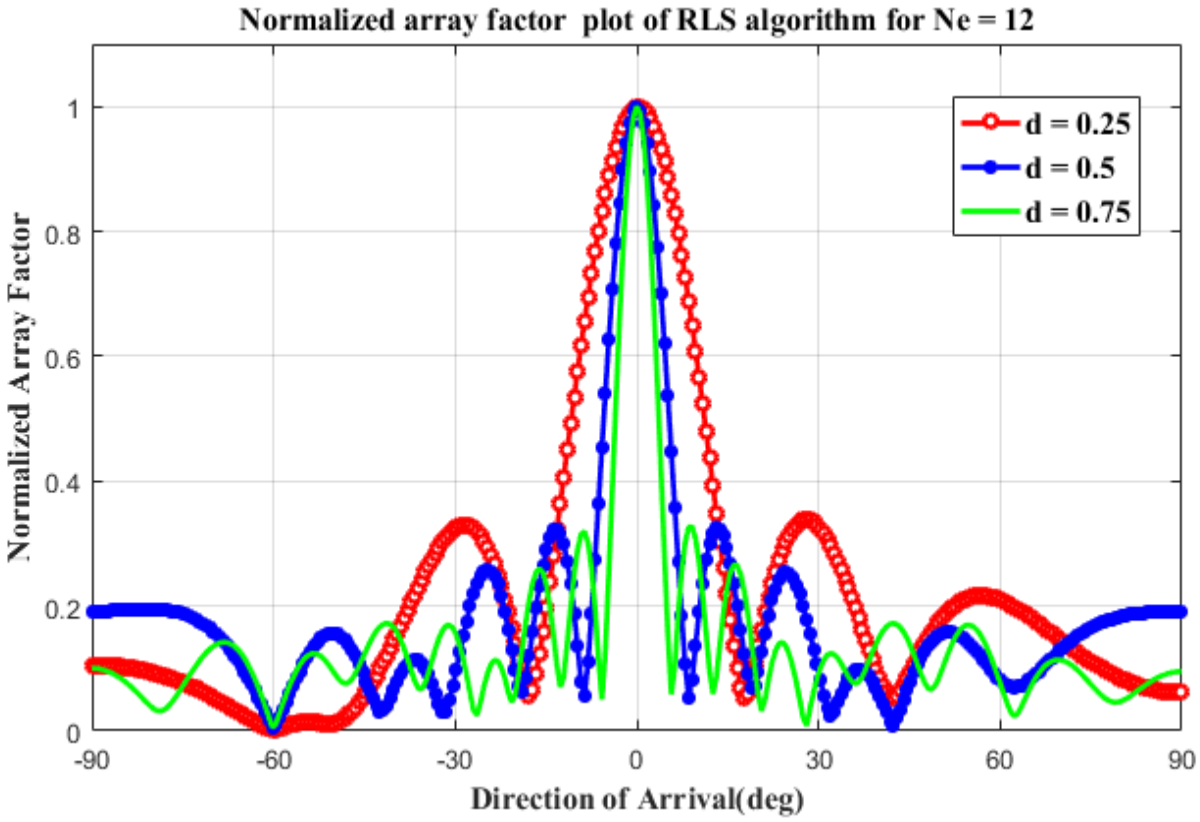

Figure 4.20: Normalized AF plots for RLS for Ne =12 and varying d at $\boldsymbol{\theta_d = 0° \; and \; \theta_i = -60°}$

From Figure 4.20, the spacng $d = 0.5\lambda$ produces a narrow beam as compared to $d = 0.25\lambda$ and has also a relatively small number of sidelobes as compared to $d = 0.75\lambda$.

The sidelobe level of the smart antenna that uses RLS as its beamforming algorithm for this thesis at θ_d= 0° and θi= -60° for different inter-element spacing and Ne = 12 can be summerized in the next table.

The table shows that, for the same number of array element Ne = 12, as the spacing d between the elements decreases there is an oscillation in the magnitude of the SLL. But when comparing the

SLL with that of the LMS algorithm, the LMS has better performance in terms of reducing radiation in undesired direction.

Table 4.5: AF SLL comparison for RLS algorithm at different element spacing & fixed Ne = 12.

DOA of desired signal (θ_d)	DOA of interferer signal (θ_i)	Inter-element spacing (d)	Number of elements in the array (Ne)	AF pattern Sidelobe level (in dB)
0°	-60°	$d = 3\lambda/4$	12	-4.85
		$d = \lambda/2$	12	-4.89
		$d = \lambda/4$	12	-4.72

4.6 Comparison of LMS, SMI and RLS algorithms on the basis of normalized AF pattern sidelobe level

This section is introduced to compare the performance of the three algorithms by plotting their normalized array factor pattern on the same graphics window of MATLAB. This helps to easily understand their performance characteristics in terms of the maximum magnitude of sidelobe which is radiation in unintended direction.

The algorithm that produces smaller magnitude of the sidelobe when considering only the maximum sidelobe magnitude is the best algorithm based on the selected criteria. The comparison is based on the magnitude of the maximum sidelobe of the array not the number of the sidelobes the array produces. For comparison purpose, only the optimum separation distance (the half wavelength) between the array elements for three different arrays is considered. This optimum inter-element spacing ($d = 0.5\lambda$) is selected because of the other two separation distances produce a broad beam ($d = 0.25\lambda$) and grating lobes ($d = 0.75\lambda$). This inter-element spacing is also selected based on the fact that increasing the spacing more than half wave length leads to large number of sidelobe even if a narrow beam is created due to large size of the array. Also for comparison purpose, the same signals for each of the three algorithms (the desired and interferer signals) are also considered.

The comparison is started by taking an array with smallest number of elements and go through the array having largest number of elements.

Case I: Comparison of LMS, SMI and RLS algorithms for Ne= 5 and $d = 0.5\lambda$

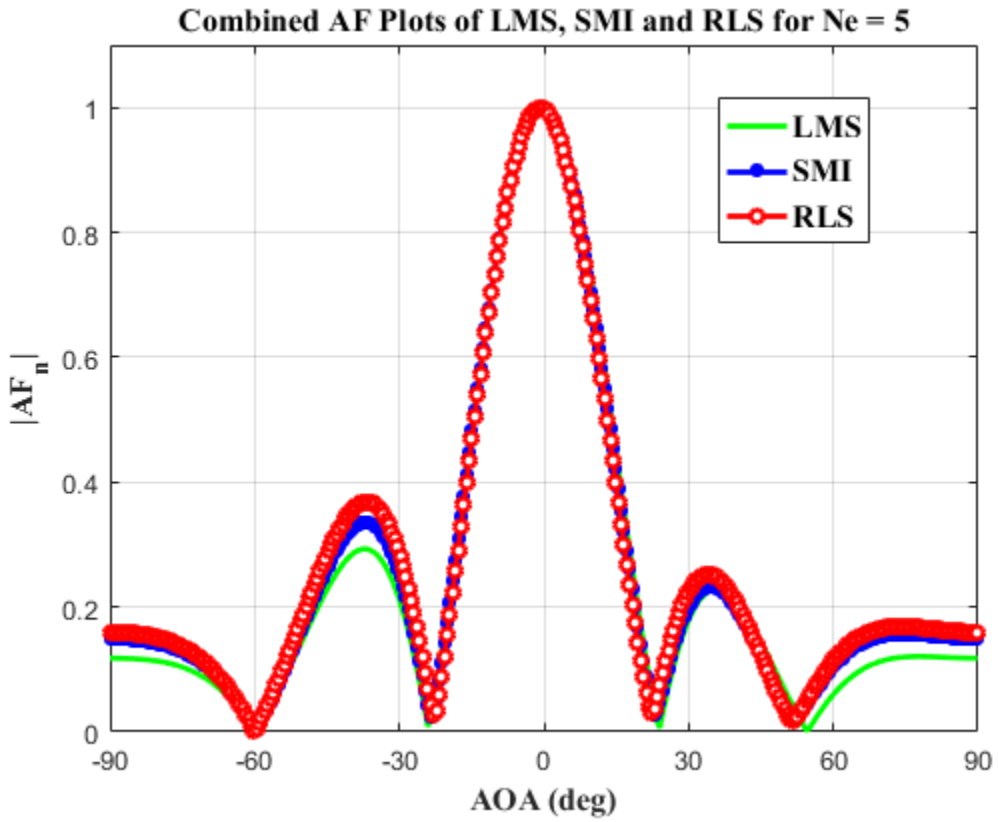

Figure 4.21: AF plot of LMS, SMI and RLS for Ne = 5 with $d = 0.5\lambda$ at $\theta_d = 0°$ and $\theta_i = -60°$

As Figure 4.21 shows, the LMS algorithm has the smallest maximum sidelobe level having almost the same main lobe and nulling characteristics with other two algorithms. The SLL for the three algorithms, for this case of the array, can be summarized in the following table.

Table 4.6: AF sidelobe comparison for LMS, SMI and RLS algorithms at $d = 0.5\lambda$ and Ne =5

DOA of desired signal (θ_d)	DOA of interferer signal (θ_i)	Inter-element spacing *(d)*	Number of elements in the array (Ne)	AF pattern SLL (in dB)		
				LMS	SMI	RLS
0°	-60°	$d = \lambda/2$	5	-5.35	-4.74	-4.34

Case II: Comparison of LMS, SMI and RLS algorithms for Ne= 8 and $d = 0.5\lambda$

Next let increase the number of elements of the array to eight and compare the SLL of the three algorithms. The plot for the three algorithms is shown in the Figure 4.22.

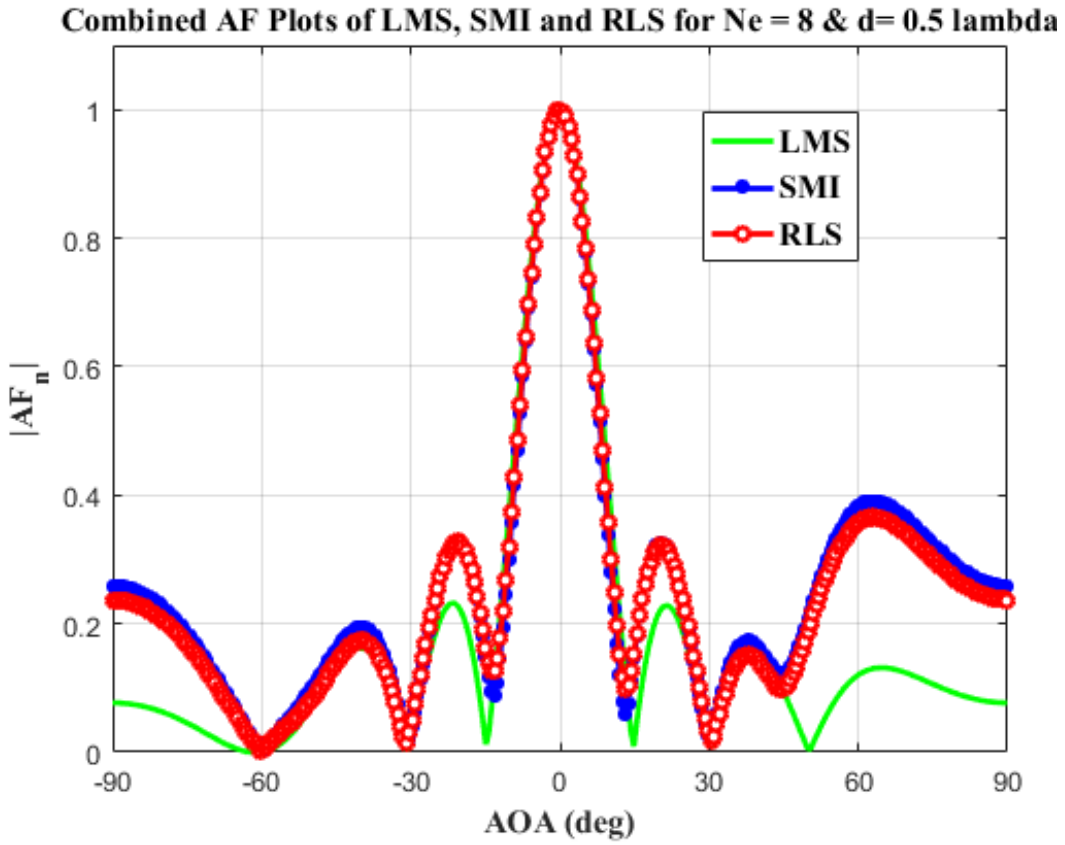

Figure 4.22: AF plot of LMS, SMI and RLS for Ne = 8 with $d = 0.5\lambda$ at $\theta_d = 0°$ and $\theta_i = -60°$

From the Figure 4.22, it is clear that, as compared to the previous one, a narrow main beam is directed towards the desired user and a deep null is placed at the interferer DOA. But in this case of array, for SMI algorithm, the plot shows a deteriorating manner in terms of SLL. Also an improved SLL reduction is gained for the LMS algorithm. The SLL for each of these methods is summarized in the following table.

Table 4.7: AF sidelobe comparison of LMS, SMI and RLS algorithms with $d = 0.5\lambda$ and Ne =8

DOA of desired signal (θ_d)	DOA of interferer signal (θ_i)	Inter-element spacing *(d)*	Number of elements in the array (Ne)	AF pattern SLL (in dB)		
				LMS	SMI	RLS
0°	-60°	$d = \lambda/2$	8	-6.34	-4.08	-4.37

Case III: Comparison of LMS, RLS and SMI algorithms for Ne = 12 and $d = 0.5\lambda$

The normalized array factor plots for the three algorithms with number of elements twelve for inter-element spacing of 0.5λ is shown in the figure below.

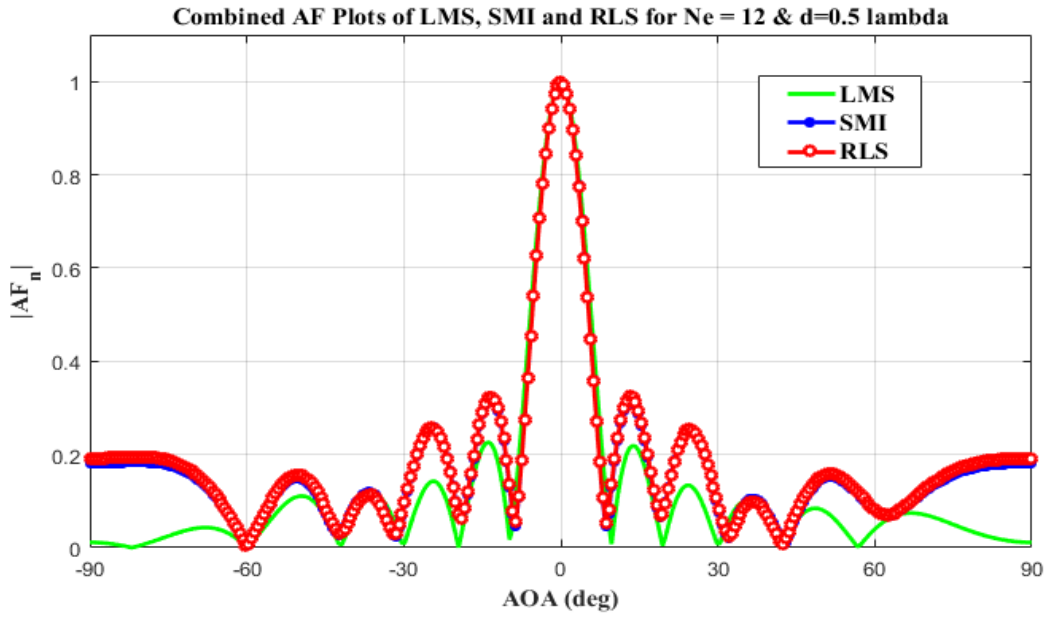

Figure 4.23: AF plot for LMS, SMI and RLS for Ne = 12 with d = 0.5λ at $\boldsymbol{\theta_d = 0°}$ and $\boldsymbol{\theta_i = -60°}$

As it is clearly investigated in Figure 4.23, a very narrow (sharp) beam can be created by increasing the number of elements of the array for the same inter-element spacing.

The SMI and RLS algorithms show almost the same characteristics of the normalized array factor plot and still the LMS algorithm play an important role in terms reducing the SLL of the array. That means better performance in reducing radiation in unintended direction is achieved by using the LMS algorithm with maximum number of elements for creating a narrow beam towards the user of interest. Table 4.8 shows a quantified value of the SLL for each of the three algorithms.

Table 4.8: AF sidelobe comparison for LMS, SMI and RLS algorithms for $d = 0.5\lambda$ and Ne =12

DOA of desired signal (θ_d)	DOA of interferer signal (θ_i)	Inter-element spacing *(d)*	Number of elements in the array (Ne)	AF pattern SLL (in dB)		
				LMS	SMI	RLS
0°	-60°	$d = \lambda/2$	12	-6.51	-4.89	-4.89

Like the other two cases, the LMS algorithm produces the lowest SLL magnitude as compared to the RLS and SMI algorithms. This property with simplest complexity at a cost of slow convergence time makes the LMS algorithm to be used in most communication systems.

Chapter 5: Conclusion and Recommendation for future work

5.1 Conclusion

For improving quality of service of wireless communication different mechanisms are introduced in different times. These mechanisms are intended for using the available resource of the spectrum efficiently and increasing the data rate while interference is minimized. One of the methods for achieving this goal of increasing the data rate (system capacity) is using the smart antenna system. The smart antenna uses beamforming algorithms for steering the main lobe in the direction of the desired user and suppresses the interferer by placing a deep null at its direction of arrival. Although the quality of communication is up graded using this type of antenna, the performance of the smart antenna depends on the type of adaptive algorithm used for its signal processing. One of the performance criteria of adaptive algorithms is reducing radiation in unintended direction. This performance criterion can be improved using an algorithm that produces lower SLL.

In this thesis work, performance analysis of three non-blind adaptive algorithms (LMS, SMI and RLS) based on sidelobe level of the AF pattern is investigated. In addition, the performance of the smart antenna on the basis of array parameters (number of elements of the array and inter-element spacing) is also discussed.

From simulation results of the thesis, there are observations that are related the array factor plots of the smart antenna that uses these three algorithms. One of the observations is that, for all the three algorithms, as the total width of the array increases the central beam becomes narrower. This is observed by taking a fixed inter-element spacing and increasing the number of elements of the array. For all of the three algorithms, a narrow beam is directed towards the user of interest when the numbers of elements of the array is large.

The second observation is that, as the inter-element spacing becomes smaller for fixed element array, a broad beam is created which leads to poor performance of smart antenna. This is observed by taking normalized array factor plot of the smart antenna for each algorithm with a single fixed element array and varying the inter-element spacing from $d = 0.75\lambda$ to 0.25λ.

Another observation, which is the main objective of this thesis, is comparative analysis of the three algorithms on the basis of SLL. Simulation results show that, the LMS algorithm has the best performance characteristics in terms of creating lower sidelobe level as compared to SMI and RLS algorithms.

5.2 Recommendation for future work

Although it has been investigated, in this thesis, the performance characteristics of smart antenna on the basis of SLL for non-blind algorithms, still there many topics which require further work. The extension of this thesis will lead to the following recommendations for further improvement in smart antenna system

- In this thesis work only non-blind adaptive algorithms are considered and further works are recommended about blind algorithms.
- For LMS algorithm, fixed step size ($\mu = 0.02$) is used through all of the simulation and using step size which is dependent up on the induced signal may lead another further work for SLL comparison.
- Flat fading channel is considered. Using other channel models leads another challenge, mitigation of these challenges for these algorithms can be extended from this work
- Only single interferer DOA is considered and when there are many interferers, improving nulling characteristics of smart antenna may be another future work.

References

[1] Io Wave Inc. (2015, October 20). *Smart Antenna (3rd ed)* [Online]. Available: http://www.iowave.com/.

[2] Dimitris G. Manolakis et al "Statistical and adaptive signal processing," McGraw Hill Publication, 2005.

[3] S. Yaser and M.A. Alem, "Performance appraisal of Smart Antennas System for Next Generation Wireless Communication," *J. of Eng. and Sci.,* January-June, 2006.

[4] G. V. Tsoulos, M. A. Beach, and S. C. Swales, "Application of Adaptive Antenna Technology to Third Generation Mixed Cell Radio Architectures," in *44th IEEE Veh. Technol. Conf.,* Vol. 1, 1994, pp. *615-619.*

[5] U. Forsse'n et al, "Adaptive Antenna Arrays for GSM 900/DCS1800," in *44th IEEE Veh. Technol. Conf.,* Vol. 1, 1994, pp. *605-609.*

[6] W. C. Y. Lee, "Applying the Intelligent Cell Concept to PCS," *IEEE Trans. Veh. Technol.*, Vol. 43, No. 3, Aug. 1994, pp. *672-679.*

[7] Somnath Patra et al, "Power pattern synthesis of smart antenna array using different adaptive algorithms," *Int. J. of Advanced Research,* Volume 3, May 2015, pp. *1459-1466.*

[8] J. Jin et al, "Array Patterns Synthesizing Using Genetic Algorithm," published in Progress in *Electromagnet. Research Symp.,* 2006, Cambridge, USA, March 26-29.

[9] T. Yuan et al, "Design and Analysis of Phased Antenna Array with Low Sidelobe by Fast Algorithm," published in Progress in *Electromagnet. Research Symp.,* PIER 87, pp. *131–147,* 2008.

[10] Ch. Santhi rani et al, "Smart Antenna Algorithms for WCDMA Mobile Communication Systems," *Int. J. of Comput. Sci. and Network Security,* Vol.8, No.7, July 2008.

[11] P. V. Subbaiah et al, "LMS and RLS Algorithms for Smart Antennas in a W-CDMA Mobile Communication Environment" *Asian Research Publishing Network J. of Eng. and Applied Sci.* Vol. 4, NO. 6, Aug. 2009.

[12] Seifu Girma, "Investigation of Adaptive Beamforming Algorithm for Smart Antenna system to Improve the Effect of Angle Separation," M.Sc. Thesis, School of Elect. And Comput. Eng., Addis Ababa Univ., Addis Ababa, Ethiopia, 2012.

[13] Paul Petrus, "Novel Adaptive Array Algorithms and Their Impact on Cellular System Capacity" Ph.D. dissertation, Dept. Elect. Eng., Faculty of the Virginia Polytechnic Institute and State University, Virginia, March 1997.

[14] F. B. Gross and I. ebrary, “Smart antennas for wireless communications with MATLAB,” McGraw-Hill, 2005.

[15] E M Al-Ardi et al, “Performance Evaluation of the LMS Adaptive Beamforming Algorithm used in Smart Antenna Systems,” *IEEE*, 2005.

[16] Lal Chand Godara, “Smart Antennas,” Boca Raton, Florida by CRC Press LLC, 2004.

[17] Tanuja S. Dhope (Shendkar), “Application of MUSIC, ESPRIT and ROOT MUSIC in DOA Estimation,”

[18] Zhigang Rong, “Simulation of Adaptive Array Algorithms for CDMA Systems,” Blacksburg, Virginia, September 1996.

[19] Zelalem Fikre Zewdu, “Performance comparison of Spatial Multiplexing and Spatial Diversity in Rate Adaptive wireless MIMO systems,” M.Sc. Thesis, School of Elect. And Comput. Eng., Addis Ababa Univ., Addis Ababa, Ethiopia, 2007.

[20] Mulugeta Atlabachew and Dr, Ing.Mohammed Abdo “Investigation of smart Antenna Beamforming for Cognitive Radio,” AAIT Technology library, December 2007.

[21] Bing-Leung and Patric Cheung “Simulation of Adaptive Array Algorithms for OFDM and Adaptive Vector OFDM Systems,” Virginia Polytechnic Institute, Virginia, September 2002.

[22] S. Haykin, "Adaptive filter theory," Prentice Hall PTR, 2002.